

Cationic α -Diimine Nickel and Palladium Complexes Incorporating Phenanthrene Substituents: Highly Active Ethylene Polymerization Catalysts and Mechanistic Studies of *syn/anti* Isomerization

Quan H. Tran, Xiqu Wang, Maurice Brookhart,* and Olafs Daugulis*



Cite This: <https://dx.doi.org/10.1021/acs.organomet.0c00696>



Read Online

ACCESS |



Metrics & More

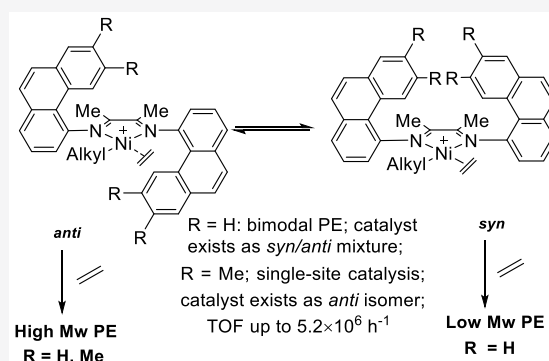


Article Recommendations



Supporting Information

ABSTRACT: α -Diimine palladium complexes incorporating phenanthryl- and 6,7-dimethylphenanthrylimino groups have been synthesized and characterized. The (diimine)PdMeCl complexes prepared from 2,3-butanedione and acenaphthenequinone bearing the unsubstituted phenanthrylimino groups, **12a** and **14a**, respectively, exist as a mixture of *syn* and *anti* isomers in a ca. 1:1 ratio. Separation and X-ray diffraction analysis of **14a-syn** and **14a-anti** isomers confirms the *syn/anti* assignments. The barrier to interconversion of **14a-syn** and **14a-anti** via ligand rotation, ΔG^\ddagger , was found to be 25.5 kcal/mol. The corresponding (diimine)PdMeCl complex prepared from acenaphthenequinone and incorporating the 6,7-dimethylphenanthrylimino group exists solely as the *anti* isomer, **14b**, due to steric crowding which destabilizes the *syn* isomer. Analogous (diimine)NiBr₂ complexes were prepared from 2,3-butanedione incorporating the phenanthrylimino group, **16a**, and the 6,7-dimethylphenanthrylimino group, **16b**. Nickel-catalyzed polymerizations of ethylene were carried out by activation of the dibromide complexes **16a,b** using various aluminum alkyl activators. Complex **16a** yields a bimodal distribution polymer, the low-molecular-weight fraction originating from the *syn* isomer and the high-molecular-weight fraction arising from the *anti* isomer. Polymerizations carried out by **16b** yield only high-molecular-weight polymers with monomodal distributions due to the existence of a single isomer (*anti*) as the active catalyst. All polymers are linear or nearly so. All catalysts are highly active, but catalysts derived from **16b** are somewhat more active than **16a** and exhibit turnover frequencies generally over 10⁶ and up to 5 × 10⁶ per hour (40 °C, 27.2 atm ethylene, 15 min). Active palladium ethylene oligomerization catalysts were generated by conversion of the neutral methyl chloride complexes **14a,b** to the cationic nitrile complexes **15a,b** via halide abstraction.



INTRODUCTION

Cationic α -diimine nickel(II) and palladium(II) complexes (Figure 1, 1a,b) showing high activity for ethylene and α -olefin polymerization were introduced in 1995. These systems produce high-molecular-weight, branched polyethylenes.¹ Such complexes are also effective catalysts for the copolymerization of ethylene with certain polar vinyl monomers.^{2,3} The critical structural feature of classical α -diimine systems is the presence of ortho aryl substituents that significantly retard the rate of chain transfer relative to the rate of chain propagation, enabling the production of high-molecular-weight polymers. Due to the approximately perpendicular arrangement of the aryl rings relative to the coordination plane of the metal, the ortho aryl substituents are positioned near axial sites above and below the five-membered chelate ring. The ortho substituents thus efficiently increase steric hindrance at metal axial positions and greatly retard the rate of polymer chain displacement by the incoming monomer.⁴ Because of the easily executed structural permutations and highly modular synthesis of the α -diimine ligands, a plethora of similar late-transition-

metal complexes have been developed for olefin polymerization over the last two decades.^{5–21} Altering ligand frameworks is used in tuning the properties of catalysts, leading to significant variations in polymerization activity as well as the microstructure of the polymer products.

In 2013, our group introduced an approach for exceptionally efficient blocking of the axial sites in nickel complexes by utilizing 8-arylnaphthyl amines which produce “sandwich”-type structures (Figure 1, 2b).²² While the substituents of traditional α -diimine catalysts point away from the coordination plane at an angle, the 8-aryl substituents are perpendicular to the naphthyl rings and are positioned over the axial sites of the complexed metal in a “sandwich-like” arrangement of the

Received: October 30, 2020

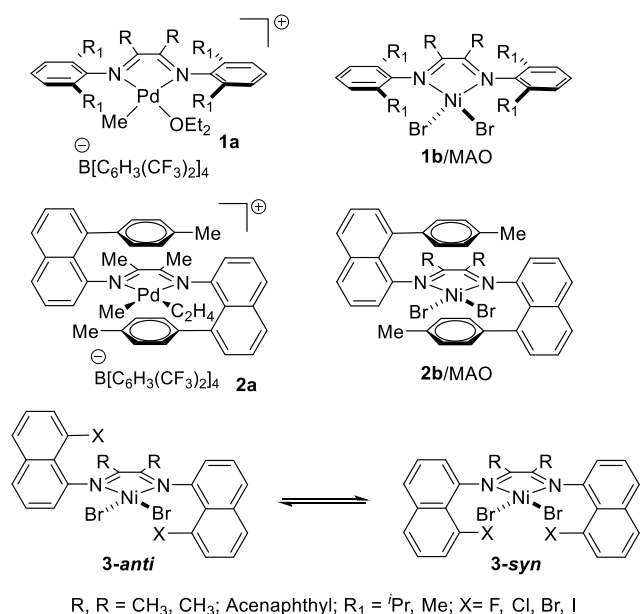


Figure 1. Group 10 metal α -diimine catalysts.

capping groups. Due to the extreme hindrance provided by the incorporation of the bulky 8-arylnaphthylimino groups, these sandwich complexes effectively inhibit displacement of the growing polymer chain. Consequently, much lower rates of chain transfer relative to rates of chain propagation are observed. The sandwich palladium catalysts (Figure 1, 2a) exhibit living polymerization behavior, generating hyperbranched polyethylene with narrow molecular weight distributions.²³ The corresponding nickel sandwich catalysts convert ethylene to an ultrahigh-molecular-weight polymer with dispersities narrower than those observed for the classical diimine systems.

Recently, we reported a series of complexes derived from 8-halonaphthalen-1-amine imines that are related to sandwich catalysts by virtue of substituting the capping aryl substituents with halogen atoms.²⁴ These complexes exist in solution as mixtures of *syn* and *anti* isomers with *syn/anti* ratios of 2/1 (X = F), 2/1 (Cl), 1/1.5 (Br), and 1/22 (I) (Figure 1, 3). The halo-substituted nickel complexes exhibit performance in ethylene polymerization dependent on the *syn/anti* ratios and their rates of interconversion. Polyethylenes produced from nickel complexes display either bimodal or broadened monomodal (X = Br) molecular weight distributions. This feature is attributed to the slower rate of interconversion of the *anti* and *syn* isomers of the active catalysts relative to the rate of polymer chain growth for all cases except when X = Br. The low-molecular-weight fraction is assigned as polyethylene formed from the *syn* isomer, whereas the *anti* isomer leads to the formation of the high-molecular-weight fraction. Nevertheless, only crystals of *syn* complexes were isolated and characterized by X-ray diffraction analysis. Interconversion of *syn/anti* isomers in tetrahedral Zn complexes derived from 8-halonaphthalen-1-amine imines exhibits barriers (ΔG^\ddagger values) in the range 16.9–19.1 kcal/mol, which is about 1–4 kcal/mol higher than barriers to migratory insertion in the nickel catalysts.

While a large number of nickel ethylene polymerization catalysts have now been developed, systems that can reach an activity level of ca. 3.6×10^6 turnovers/h (or ca. 10^8 g mol⁻¹

h⁻¹) remain rare. The classical α -diimine nickel complex (Figure 1, 1b; R, R = acenaphthyl) exhibits an average polymerization activity of 3.7×10^6 h⁻¹ in a 10 min run at 35 °C.²⁵ Similar activities were obtained for the nickel(II) triadamantylphosphine²⁶ and α -iminoketone²⁷ catalysts in about 3 min runs (Figure 2, 4 and 5). The highest

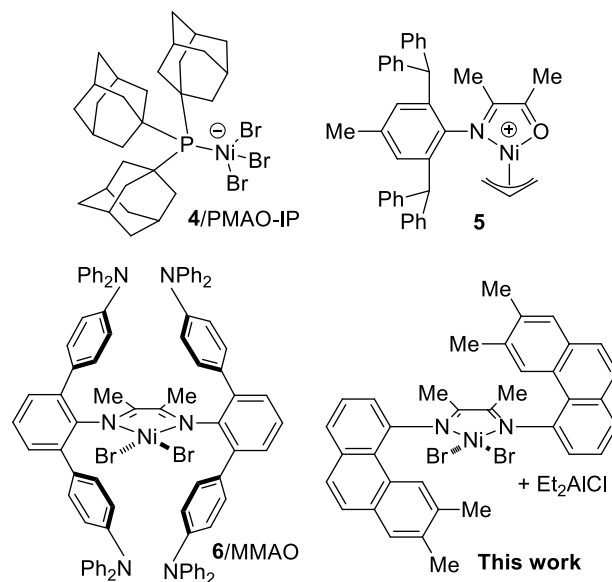


Figure 2. Highly active nickel-based ethylene polymerization catalysts.

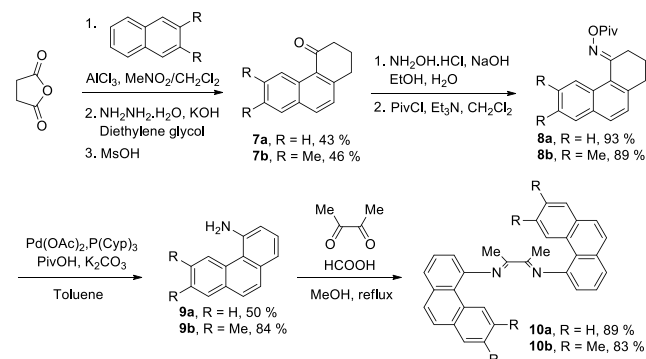
polymerization activity provided by a nickel system was observed using a cationic nickel α -diimine catalyst modified with (4-diphenylamino)phenyl substituents (Figure 2, 6).²⁸ An ultrahigh activity of 37×10^6 h⁻¹ was achieved in a 1 min reaction. These notably high catalytic activities were obtained over very short reaction times, eliminating any deleterious effects of short catalyst lifetimes.

We report here the preparation, characterization, and ethylene polymerization activities of new nickel and palladium complexes derived from phenanthryl- and 6,7-dimethylphenanthryl- α -diimines. A nickel complex prepared from 6,7-dimethylphenanthrylamine shows a very high activity level of 4.4×10^6 h⁻¹ for ethylene polymerization in a 30 min run.

RESULTS AND DISCUSSION

Synthesis of Diimine Ligands. The preparation of α -diimine ligands 10a,b is presented in Scheme 1. Friedel–Crafts acylation of naphthalene and 2,3-dimethylnaphthalene gave the

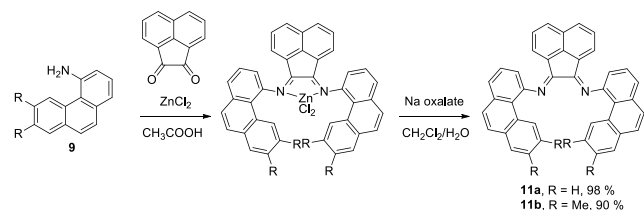
Scheme 1. Synthesis of 2,3-Butanedione Diimines



corresponding keto acids that subsequently underwent a Wolff–Kishner reduction followed by cyclization to provide dihydrophenanthren-4(1*H*)-ones **7a,b**. Conversion of **7a,b** to oximes followed by pivaloylation gave **8a,b**. Subsequent Pd-catalyzed Semmler–Wolff-type reactions afforded aminophenanthrenes **9a,b**. The α -diimine ligands **10a,b** were readily prepared by the reaction of 2,3-butanedione with the aminophenanthrenes in MeOH in the presence of a catalytic amount of formic acid. While ligand **10a** shows good solubility in methylene chloride, ligand **10b** is nearly insoluble in most common solvents, including toluene, methanol, diethyl ether, and methylene chloride.

The corresponding α -diimine ligands **11a,b** derived from acenaphthenequinone were prepared by using the $ZnCl_2$ -template method (Scheme 2).²⁹ The reactions of amino-

Scheme 2. Synthesis of Acenaphthenequinone Diimines

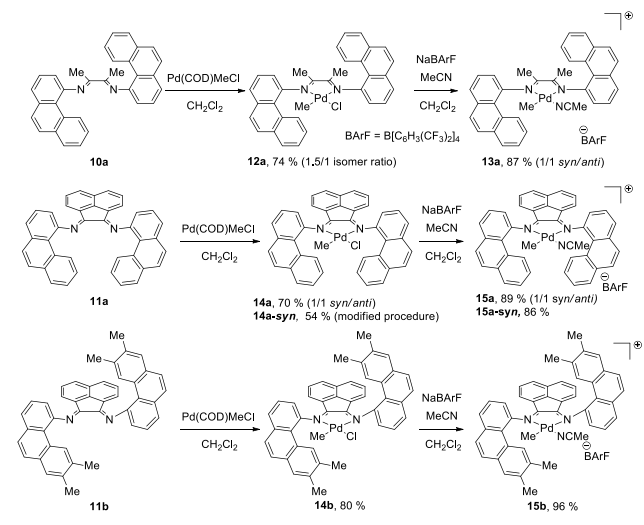


phenanthrenes with acenaphthenequinone in the presence of $ZnCl_2$ gave the diimine zinc complexes as dark red solids. Decomplexation of zinc chloride with sodium oxalate provided free ligands **11a,b** as red powders. These ligands display good solubility in methylene chloride. All of the ligands were characterized by 1H and ^{13}C NMR spectroscopy as well as high-resolution mass spectroscopy (HRMS).

Synthesis and Structure of Palladium Complexes.

The preparation of the palladium complex **12a** is shown in Scheme 3. Displacement of COD from $Pd(COD)MeCl$ by

Scheme 3. Synthesis of Palladium Complexes



ligand **10a** generated deep red **12a** in high yield. Complex **12a** is slightly soluble in methylene chloride and nearly insoluble in toluene and pentane. The 1H NMR spectrum of **12a** in methylene chloride- d_2 shows two singlet resonances centered at 0.48 (major) and 0.45 ppm (minor) in a 1.5/1 ratio that are assigned as the signals of Pd-bound methyl groups.

Considering the analogy with **3** (Figure 1), the most likely explanation is that complex **12a** exists as a 1.5/1 *syn/anti* mixture. The reaction of ligand **10b** with $Pd(COD)MeCl$ in methylene chloride did not lead to a pure diimine-palladium complex, presumably due to the poor solubility of **10b**.

Ligands **11a,b** react with $Pd(COD)MeCl$ to afford respectively palladium complexes **14a,b** in good yields (Scheme 3). Similar to **12a**, a nearly 1/1 equilibrium mixture of *syn/anti* conformers of complex **14a** was observed by 1H NMR spectroscopy, as was evident by the presence of two signals for the palladium-bound methyl groups centered at 0.78 and 0.74 ppm. The structure of each isomer of **14a** was confirmed by a single-crystal X-ray diffraction analysis, and their structures are shown in Figures 3 and 4. The *syn* and *anti*

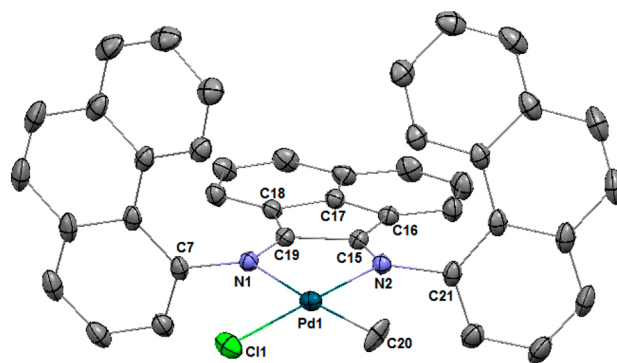


Figure 3. Molecular structure of palladium complex **14a-syn**. Hydrogen atoms are omitted for clarity. Thermal ellipsoids are shown at the 50% probability level. Selected bond lengths (Å) and angles (deg): C20–Pd1 2.053(2); Pd1–N1 2.1874(19); Pd1–N2 2.058(2); Pd1–Cl1 2.289(7); C20–Pd1–N1 174.42(11); C20–Pd1–N2 94.96(11); N1–Pd1–N2 79.45(8); C20–Pd1–Cl1 87.52(9).

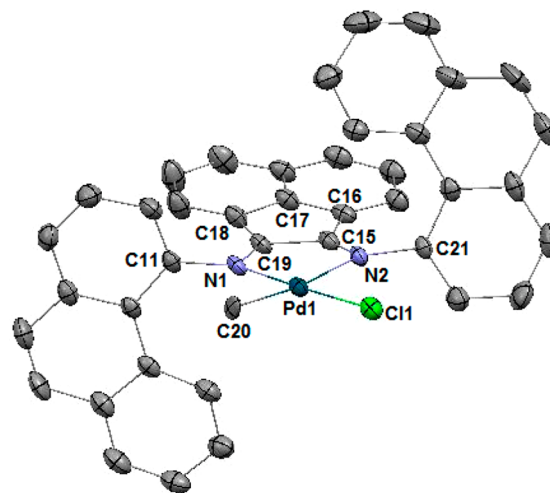
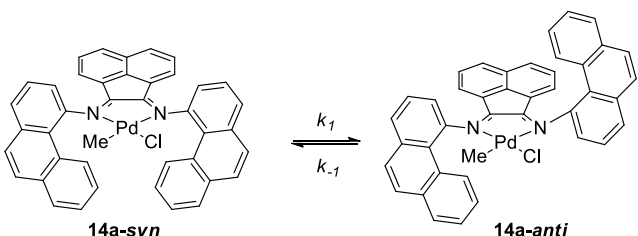


Figure 4. Molecular structure of palladium complex **14a-anti**. Hydrogen atoms are omitted for clarity. Thermal ellipsoids are shown at the 50% probability level. Selected bond lengths (Å) and angles (deg): C20–Pd1 2.039(4); Pd1–N1 2.054(3); Pd1–N2 2.177(3); Pd1–Cl1 2.2920(11); C20–Pd1–N1 93.21(15); C20–Pd1–N2 171.46(14); N1–Pd1–N2 79.20(12); C20–Pd1–Cl1 89.63(13).

conformers crystallize separately, and crystal picking was used to collect each isomer. As expected, a square-planar geometry is exhibited at the palladium center. In the single crystal of complex **14a-syn**, two phenanthrene rings face each other, shielding only one axial position of the coordination site (Figure 3). In contrast, complex **14a-anti** contains two phenanthrene rings that shield the axial sites above and below the palladium center (Figure 4). Remarkably, **14a-syn** could be isolated in pure form (>30/1 *syn/anti*) using a modified synthetic procedure. After overnight stirring of **11a** with Pd(COD)MeCl in methylene chloride, toluene was added to the reaction mixture and the resulting mixture was carefully evaporated at 60 °C until a precipitate formed. **14a-syn** was collected by filtration as a red solid. The identity of the product was verified by NMR spectroscopy, showing a nearly pure *syn* isomer.

As was established earlier, activation with organoaluminum cocatalysts in the presence of ethylene yields square-planar cationic nickel catalysts that structurally resemble the corresponding palladium complexes.^{30–33} The existence of palladium complexes **12a** and **14a** as a *syn/anti* mixture of isomers suggests that the behavior of the nickel complexes in polymerization could be complicated. Since the investigation of the paramagnetic nickel dibromide complexes is problematic, and square-planar Ni(II) catalytic intermediates are expected to be unstable, an analysis of the model palladium complex **14a** was conducted. In solution, **14a-syn** converts to **14a-anti**, forming an equilibrium mixture of isomers. The rate of isomerization of **14a-syn** was investigated using NMR spectroscopic analysis in tetrachloroethane-*d*₂. The data are presented in Table 1. At 313 K, **14a-syn** very slowly isomerizes

Table 1. Rates and Activation Parameters for *syn–anti* Interconversion of **12b**



temp (K)	$k_{\text{obs}} = k_1 + k_{-1}$ (10^{-5} s^{-1})	k_1 (10^{-5} s^{-1})	k_{-1} (10^{-5} s^{-1})
313	2.07 ± 0.01	0.92 ± 0.02	1.15 ± 0.03
323	8.10 ± 0.25	3.60 ± 0.11	4.50 ± 0.14
333	29.6 ± 0.82	13.2 ± 0.36	16.4 ± 0.46
343	77.2 ± 3.99	34.8 ± 1.77	43.4 ± 2.21

Activation Parameters	
$\Delta G_{298\text{K},1}^\ddagger = 25.5 \pm 0.1 \text{ kcal/mol}$	$\Delta G_{298\text{K},-1}^\ddagger = 25.4 \pm 0.1 \text{ kcal/mol}$
$\Delta H_1^\ddagger = 25.4 \pm 0.9 \text{ kcal/mol}$	$\Delta H_{-1}^\ddagger = 25.4 \pm 0.9 \text{ kcal/mol}$
$\Delta S_1^\ddagger = -0.43 \pm 2.8 \text{ cal/mol}$	$\Delta S_{-1}^\ddagger = -0.03 \pm 2.8 \text{ cal/mol}$

to **14a-anti**, resulting in a nonequilibrium ratio of 2.5/1 *syn/anti* after 12 h. An increase in temperature facilitates the isomerization. The equilibrium ratio of 1.25/1 *syn/anti* was achieved after 2 h at 343 K. Using a reversible first-order kinetic analysis, the rate constants, k_1 and k_{-1} , were obtained from the k_{obs} ($k_1 + k_{-1}$) value and the equilibrium constant, $k_1/k_{-1} = 0.8$. An Eyring analysis of the rate data between 313 and 343 K gave the activation parameters. The barrier to isomerization between *syn* and *anti* isomers in palladium

complex **14a** is 25.5 kcal/mol. The contribution of activation entropies to the free energies of activation is very small, as expected. For comparison, interconversion between *syn* and *anti* isomers in zinc 8-halonaphthyl- α -diimine complexes proceeds with much lower barriers of 16.9–19.1 kcal/mol.²⁴

In contrast to the palladium complexes derived from phenanthrene, complex **14b** containing 6,7-dimethyl substituents exists as a single conformer. The ¹H NMR spectrum of **14b** in methylene chloride-*d*₂ contains only one set of resonances. The structure of complex **14b** was verified by a single-crystal X-ray diffraction analysis after recrystallization by layering pentane over a solution of **14b** in methylene chloride at room temperature. The molecular structure of **14b** is shown in Figure 5. Complex **14b** crystallizes in triclinic space group

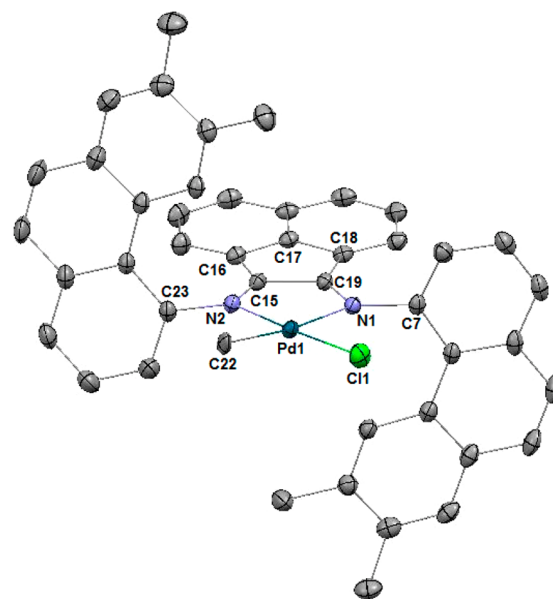


Figure 5. Molecular structure of palladium complex **14b**. Hydrogen atoms are omitted for clarity. Thermal ellipsoids are shown at the 50% probability level. Selected bond lengths (Å) and angles (deg): Pd1–C22 2.0545(11); Pd1–N2 2.0604(12); Pd1–N1 2.1829(12); Pd1–Cl1 2.2768(4); C22–Pd1–N2 94.67(6); C22–Pd1–N1 172.63(5); N2–Pd1–N1 79.12(5); C22–Pd1–Cl1 89.03(5).

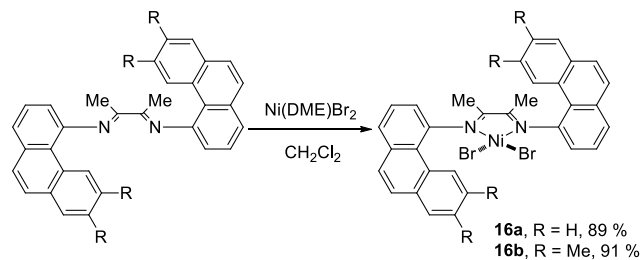
P1 and shows a square-planar geometry around the palladium center in the solid state. As anticipated, the sterically bulky methyl groups force the palladium complex **14b** to adopt an *anti* conformation. The two dimethyl-substituted phenanthrene rings effectively cap the axial sites of the square-planar coordination plane of palladium.

The acetonitrile-ligated palladium complexes **13a**, **15a**, and **15b** were obtained in high yield via halide abstraction from the corresponding complexes **12a**, **14a**, and **14b**, respectively, using NaBARF in the presence of acetonitrile (Scheme 3). These nitrile complexes were characterized by ¹H and ¹³C NMR spectroscopy and HRMS. Similar to those observed with palladium methyl chloride complexes, the nitrile complexes decorated with unsubstituted phenanthryl groups gave a *syn/anti* mixture of isomers and the nitrile complex bearing dimethyl-substituted phenanthryl groups was obtained as a single isomer. The palladium complex **15a-syn** was prepared from **14a-syn** at 0 °C.

Synthesis of Nickel Dibromide Complexes. The reaction of ligands **10a,b** with (DME)NiBr₂ in methylene

chloride at room temperature led to the formation of brick red nickel(II) dibromide complexes **16a,b** in excellent yields (Scheme 4). These paramagnetic nickel complexes exhibit poor solubility in common organic solvents such as toluene, diethyl ether, and methylene chloride.

Scheme 4. Synthesis of Nickel Complexes



Ethylene Polymerization by Nickel Complexes. Ethylene polymerizations were carried out by the activation of nickel(II) dibromide precatalysts **16a,b** in toluene using organoaluminum compounds in a 2500/1 Al/Ni ratio. The reaction is very exothermic, and low catalyst loadings were used to efficiently maintain the reaction temperature and to minimize the effect of mass-transport issues due to precipitation of the polymer. Under 13.6–40.8 atm of ethylene the reactions proceed to yield linear to lightly branched polyethylenes. Turnover frequencies (TOFs) were calculated as (mol of ethylene converted to polymer)/((mol of Ni) time). As a consequence, they represent an average TOF over the polymerization time. Polymer branching densities were obtained by a ^1H NMR spectroscopic analysis. Polymerization results are presented in Tables 2 and 3.

Table 2 summarizes the behavior of phenanthrene-derived nickel complex **16a** in polymerizations. Cocatalysts greatly influence the activity of complex **16a** and the microstructure of the resulting polyethylene. All of the organoaluminum compounds are effective cocatalysts. Upon activation by aluminum-based cocatalysts, complex **16a** displays high activity at 13.6 atm of ethylene pressure and 25 °C with TOFs over 30 min ranging from 0.14×10^6 to 1.00×10^6 h $^{-1}$. The catalyst activities increase in the order $i\text{-Bu}_3\text{Al} < \text{PMAO-IP} < \text{MMAO} < \text{Et}_2\text{AlCl} < \text{EtAlCl}_2$. In all cases, nearly linear polyethylenes with 1–3 branches per 1000 C are produced, with melting temperatures of ca. 130 °C.

The most remarkable feature of complex **16a** is the production of polyethylenes with a bimodal distribution of

molecular weights that is strongly dependent on the cocatalyst. When modified methylaluminoxane MMAO-3A is used (Table 2, entries 1–3), two elution peaks are observed in gel permeation chromatography (GPC). A minor fraction of high-molecular-weight polyethylene is detected with $M_p = 76$ kg/mol along with a major fraction of low-molecular-weight polyethylene with $M_p = 7.7$ kg/mol (entry 1). When both fractions are considered, a broad molecular weight distribution (MWD) of 5.2 is calculated (see Figure S6 in the Supporting Information). When the ethylene pressure is increased from 13.6 to 27.2 atm, the TOF increases only by a factor of 1.24, from 0.66×10^6 to 0.82×10^6 h $^{-1}$ and a bimodal molecular weight distribution is again observed (entry 2; Figure S7). An increase of temperature from 25 to 40 °C leads to a significant increase in TOF (from 0.82×10^6 to 1.89×10^6 h $^{-1}$, entry 3) and again a bimodal distribution is observed with a MWD of 6.6 (Figure S8). The branching density increases and the melting temperature decreases with increasing polymerization temperature, as is commonly observed using other nickel catalysts.^{22,24} Specifically, complex **16a** produces nearly linear polyethylene (1 branch per 1000 C) at 25 °C, and lightly branched polyethylene (9 branches per 1000 C) at 40 °C. The increase in branching with an increase in temperature is commonly ascribed to an increase in the rate of chain walking relative to the rate of chain growth.²² Similar to the case for MMAO-3A, the use of PMAO-IP activator also produces polyethylene with a relatively high M_w/M_n of 5.9 when the reaction is run at 25 °C and 13.6 atm of ethylene, showing a bimodal polymer distribution (entry 4; Figure S9). Since the related palladium complexes **12a** and **14a** exist as isomeric mixtures, it is likely that the nickel(II) dibromide precatalyst **16a** is activated by aluminum-based cocatalysts to generate the active nickel species as a mixture of the *syn* and *anti* isomers (17-*syn*/17-*anti*), as shown in Scheme 5. The *anti* complex will generate the minor high-molecular-weight polymer fraction, and the *syn* isomer will form the major low-molecular-weight fraction. As was established in previous studies, the key aspect to obtain a high-molecular-weight polymer is effective axial shielding that considerably retards the rate of chain transfer over the rate of chain propagation. In the case of the *syn* conformer, only one axial position is capped, resulting in an increased rate of chain transfer. Consequently, low-molecular-weight polyethylene is produced. In contrast, the *anti* isomer possesses two phenanthrene groups that are capable of efficiently shielding axial sites above and below the coordination plane; thus, high-molecular-weight polyethylene

Table 2. Ethylene Polymerizations Using Activated Nickel Complex 16a

entry ^a	activator	temp (°C)	pressure (atm)	TOF (10 ⁶ h ⁻¹)	M_n^b (kg/mol)	M_w/M_n	M_p (kg/mol)	branches ^c (/1000 C)	T_m^d (°C)
1	MMAO-3A	25	13.6	0.66	7.8	5.2	76.0/7.7	1	130.0
2	MMAO-3A	25	27.2	0.82	4.5	7.2	60.3/5.7	3	130.4
3	MMAO-3A	40	13.6	1.89	2.9	6.6	30.7/3.6	9	122.7
4	PMAO-IP	25	13.6	0.56	9.2	5.9	73.0/10.1	2	130.0
5	$i\text{Bu}_3\text{Al}$	25	13.6	0.14	12.5	4.0	52.5/19.7	3	130.9
6	Et_2AlCl	25	13.6	0.76	8.8	3.4	13.0 ^e	3	130.5
7	EtAlCl_2	25	13.6	1.00	9.5	3.0	15.1 ^e	3	130.4
8	EtAlCl_2	25	27.2	0.95	7.2	2.0	8.9 ^e	3	130.8
9	EtAlCl_2	40	13.6	1.76	10.6	2.8	15.7 ^e	12	120.9

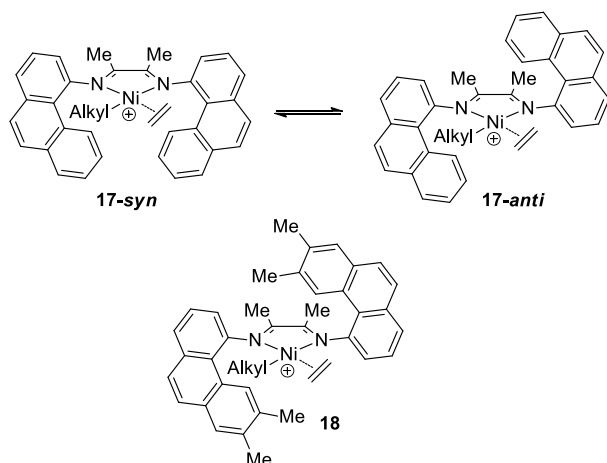
^aConditions: Ni (0.2 μmol), activator (0.5 mmol), toluene (150 mL), 0.5 h. ^bAbsolute molecular weight determined by GPC in 1,2,4-trichlorobenzene. ^cBranching numbers per 1000 carbons determined by ^1H NMR spectroscopy. ^d T_m determined by DSC. ^eLow-molecular-weight peak with a high-molecular-weight shoulder.

Table 3. Ethylene Polymerizations Using Activated Nickel Complex 16b

entry ^a	activator	temp (°C)	pressure (atm)	TOF (10 ⁶ h ⁻¹)	M _n ^b (kg/mol)	M _w /M _n	branches ^c (/1000 C)	T _m ^d (°C)
1	MMAO-3A	25	13.6	1.09	72	2.2	3	132.1
2	PMAO-IP	25	13.6	1.05	96	2.2	1	131.8
3	EtAlCl ₂	25	13.6	0.48	122	2.0	3	130.3
4	Et ₂ AlCl	25	13.6	1.58	121	1.9	2	131.0
5	Et ₂ AlCl	25	27.2	1.63	134	1.7	2	131.9
6	Et ₂ AlCl	40	27.2	4.43	39	2.0	10	121.7
7 ^e	Et ₂ AlCl	40	27.2	5.16	48	2.0	7	125.2
8 ^e	Et ₂ AlCl	40	40.8	5.14	70	1.8	6	125.5
9	Et ₂ AlCl	60	27.2	2.74	28	1.8	15	116.8

^aConditions unless specified otherwise: Ni (0.2 μmol), activator (0.5 mmol), toluene (150 mL), 0.5 h. ^bAbsolute molecular weight determined by GPC in 1,2,4-trichlorobenzene. ^cBranching numbers per 1000 carbons determined by ¹H NMR spectroscopy. ^dT_m determined by DSC. ^e15 min.

Scheme 5. Interconversion of *syn*/*anti* Isomers in a Ni Alkyl Ethylene Intermediate



is formed. The observation of a bimodal distribution of molecular weight indicates that the rate of interconversion of *syn*/*anti* isomers is slower than the rate of formation of a single chain. If a rapid interconversion were taking place, a monomodal GPC trace would be observed. The behavior of complex **16a** is consistent with that seen for nickel α -diimine catalysts generated from 8-halo-1-naphthylamines²⁴ and from unsymmetrical ligands.^{34,35}

The use of other cocatalysts including *i*Bu₃Al, Et₂AlCl, and EtAlCl₂ (Table 2, entries 5–7; Figures S10–12) decreases the molecular weight distributions to 4.0, 3.4, and 3.0, respectively. Low-molecular-weight polyethylenes were found to be the major fraction, consistent with the data observed for MMAO-3A and PMAO-IP. Notably, at 25 °C and 27.2 atm of ethylene, complex **16a** activated by EtAlCl₂ produces polyethylene with a M_w/M_n value of 2.0 (entry 8, Figure S13). A low-MW polymer with an M_n value of 7.2 kg/mol was obtained. An increase in temperature from 25 to 40 °C leads to a ca. 2-fold increase in TOF from 1.00 × 10⁶ to 1.76 × 10⁶ h⁻¹, and polyethylene with 12 branches per 1000 C and a T_m value of 120.9 was obtained (entry 9, Figure S14).

Table 3 shows polymerization results upon activation of nickel(II) dibromide **16b** containing dimethylphenanthryl substituents. Complex **16b** forms highly active catalysts upon activation by various aluminum-based cocatalysts and exhibits single-site catalytic behavior, allowing for the formation of polyethylenes with molecular weight distributions in the range of 1.7–2. In contrast to the active Ni species **17**, it is likely that the active dimethyl-substituted complex **18** exists as the *anti*

isomer exclusively, thus affording high-molecular-weight, monomodal polyethylenes (Scheme 5).

In most of the cases, the activity of activated **16b** is noticeably higher than that of **16a**. For example, upon activation by MMAO-3A, **16b** displays a TOF at a 13.6 atm ethylene pressure of 1.09 × 10⁶ h⁻¹ in comparison to the TOF of 0.66 × 10⁶ h⁻¹ observed for **16a** under similar conditions (Table 2, entry 1 vs Table 3, entry 1). A similar TOF is obtained using PMAO-IP as an activator (entry 2). Polymers formed with either MMAO-3A or PMAO-IP activators possess high molecular weights in the range of 72–96 kg/mol and branching densities of less than 5 branches per 1000 C. EtAlCl₂ is also a competent activator, albeit the activities observed are lower. Linear high-molecular-weight polyethylene with an M_n value of 122 kg/mol and 3 branches per 1000 C (entry 3) was obtained.

The best results were obtained by employing Et₂AlCl as an activator. Under these conditions, activated complex **16b** not only exhibits higher productivity than complex **16a** (TOF = 1.58 × 10⁶ h⁻¹ vs 0.76 × 10⁶ h⁻¹; entry 4, Table 3, vs entry 6, Table 2) but also produces high-molecular-weight polyethylene with M_n = 121 kg/mol. Consequently, Et₂AlCl was used as an activator in all other runs. At 25 °C, increasing the ethylene pressure from 13.6 to 27.2 atm had little effect on the TOFs observed in 30 min runs (Table 3, entries 4 and 5). The same situation was observed at 40 °C when the pressure was increased from 27.2 atm (entry 7) to 40.8 atm (entry 8). Turnover frequencies stayed about the same at ca. 5.2 × 10⁶ h⁻¹. These results suggest that the catalyst resting state is likely the alkyl ethylene species **18**, which would show no dependence of TOF on ethylene pressure.

Average TOFs are appreciably dependent on polymerization temperature. An increase in temperature from 25 to 40 °C leads to approximately 3-fold increase in TOF in 30 min runs, from 1.63 × 10⁶ to 4.43 × 10⁶ h⁻¹ (Table 3, entries 5 and 6). A high TOF of 2.74 × 10⁶ h⁻¹ could be achieved even at 60 °C (entry 9). The experimental results show that the activity remains at high levels over 30 min, revealing a relatively good stability of the catalyst derived from complex **16b**. For comparison, the TOF determined for the tri-1-adamantylphosphine-nickel complex **4** is 3.7 × 10⁶ h⁻¹ at 10 °C and 27.2 atm of ethylene, measured over 3.5 min.²⁶ The TOFs substantially dropped with even a minor lengthening of the reaction time. Similarly, Zhang and Jian described α -diimine that by using (4-diphenylamino)phenyl-modified α -diimine nickel catalyst **6**, an ultrahigh activity of 37 × 10⁶ h⁻¹ could be achieved when the reaction was carried out for 1 min.²⁸ The classical α -diimine²⁵ and α -iminoketone²⁷ nickel catalysts (Figure 1, **1b**,

and Figure 2, S) gave activities of $3.7 \times 10^6 \text{ h}^{-1}$ over 10 and 3 min, respectively. Previously reported high catalytic activities were stated for relatively short reactions, while the current catalyst remains highly active in substantially longer runs. This feature may be important for practical applications.

At 15 min, complex **16b** exhibits a slightly higher TOF of $5.16 \times 10^6 \text{ h}^{-1}$ and gives polyethylene with an M_n value of 48 kg/mol (entry 7). At increased temperatures, the polymer microstructure is altered from linear to lightly branched and the molecular weight decreases. For example, complex **16b** at 27.2 atm produces polyethylene with an M_n value of 134 kg/mol and 2 branches per 1000 carbons, while at 60 °C the polymer exhibits an M_n value of 28 kg/mol and 15 branches per 1000 C.

Ethylene Oligomerization with Palladium Complexes. The catalytic behavior of palladium complexes was explored at room temperature in methylene chloride solution under 13.6 atm of ethylene. Somewhat unexpectedly, palladium catalysts showed behavior remarkably distinct from that of nickel complexes. The results are summarized in Table 4.

Table 4. Oligomerization by Palladium Complexes

entry ^a	catalyst	time (h)	pressure (atm)	TOF (h ⁻¹)	M_n (g/mol)
1	13a	48	13.6	190	530
2	15a	20	13.6	150	250
3	15a-syn	20	13.6	170	260
4	15b	20	13.6	130	630

^aConditions: Pd catalyst (10 μmol), ethylene (13.6 atm), CH₂Cl₂ (50 mL), 25 °C. M_n was determined by ¹H NMR spectroscopy. Oligomers contain 90–110 branches/1000 C.

While the substantially lower activity of complexes **13a** and **15a,b** was anticipated, only low-molecular-weight oligomers were produced. Turnover frequencies are comparable to those observed using “sandwich” palladium catalysts.²³ The more hindered catalyst **15b** bearing dimethyl-substituted phenanthryl groups exhibits a TOF of 130 h⁻¹. The decreased steric hindrance in phenanthrene-derived catalysts **13a** and **15a** resulted in slightly higher TOFs and a concurrent reduction in oligomer molecular weight. No significant difference between an oligomerization behavior of **15a-syn** and a **15a-syn/-anti** mixture was observed (entries 2 and 3).

CONCLUSIONS

The synthesis and use as polymerization catalysts of nickel and palladium complexes incorporating phenanthrene substituents on ligands is described. The cationic α -diimine nickel and palladium complexes incorporating unsubstituted phenanthrylimino groups exist as mixtures of *syn* and *anti* isomers. Crystals of both *syn* and *anti* isomers of acenaphthenequinone-derived palladium complex **14a** were analyzed by an X-ray diffraction analysis. Pure **14a-syn** was obtained and used to investigate the *syn/anti* isomerization. The energy barrier to *syn/anti* isomerization in **14a** is 25.5 kcal/mol, as established by kinetic analysis using NMR spectroscopy at various temperatures. The ethylene polymerization behavior of nickel complex **16a** depends on the organoaluminum cocatalyst. Upon activation by MMAO-3A or PMAO-IP, the nickel complex **16a** polymerizes ethylene to yield a polymer with a bimodal distribution of molecular weight. The bimodal molecular weight distribution is ascribed to the presence of catalytically

active *syn/anti* isomers. Two phenanthryl rings of the *syn* isomer are situated at the same side of the coordination plane and block one axial site of the metal center. Consequently, polyethylene produced by the *syn* isomer has relatively low molecular weight. The *anti* isomer in which both axial sites are blocked generates polyethylene with high molecular weight. Surprisingly, the use of EtAlCl₂ activator results in the generation of largely low-molecular-weight polyethylene. It is not clear how the nature of the cocatalysts influences the molecular weight distributions of the polymers.

Nickel and palladium complexes bearing more hindered 6,7-dimethylphenanthryl substituents exist as single isomers. An X-ray diffraction study of palladium complex **14b** confirms the *anti* orientation of the 6,7-dimethylphenanthryl groups and indicates axial shielding more extensive than that observed in complex **14a**. Nickel complex **16b** is anticipated to adopt a similar conformation and produces linear to lightly branched polyethylenes with molecular weight distributions of ca. 2 and M_n values of ca. 72–134 kg/mol at 25 °C. At 40 °C and 27.2 atm of ethylene, complex **16b** exhibits an average TOF of $5.16 \times 10^6 \text{ h}^{-1}$ over 15 min. Notably, the catalytic activity is capable of remaining at a very high level of $4.43 \times 10^6 \text{ h}^{-1}$ when the reaction is carried out for 30 min. Previous examples of similar catalytic activities by nickel diimine complexes were observed at short reaction times, typically 10 min or less.

EXPERIMENTAL SECTION

General Materials and Methods. All procedures were carried out under a nitrogen atmosphere using standard glovebox and Schlenk techniques unless otherwise noted. Diethyl ether, pentane, methylene chloride, and toluene were purified by an JC Meyer solvent purification system. Column chromatography was performed on 60 Å silica gel (SiliCycle Inc.) using EtOAc/hexanes mixtures as eluents. The ¹H, ¹³C, and ¹⁹F NMR spectra were recorded on a JEOL EC-400, JEOL EC-500, or JEOL EC-600 spectrometer using the residual solvent peak as a reference. Analytical thin-layer chromatography was performed on silica gel TLC Al foils with a fluorescent indicator (254 nm) from SiliCycle Inc. Compounds for HRMS were analyzed by positive mode electrospray ionization (CI or ESI) using an Agilent QTOF mass spectrometer in the Mass Spectrometry Facility (MSF) of the Department of Chemistry and Biochemistry of the University of Texas Austin. Elemental analyses were performed by Atlantic Microlabs Inc. (Norcross, GA, USA). Reagents and starting materials were obtained from commercial sources and used without further purification unless otherwise noted. MMAO-3A (7 wt % solution in heptane) and PMAO-IP (7 wt % solution in toluene) were purchased from AkzoNobel. EtAlCl₂ (1.8 M solution in toluene) was purchased from Acros. Et₂AlCl (25 wt % solution in toluene) was purchased from Sigma-Aldrich. Polymerization reactions were carried out in a Parr 450 mL mini reactor with Matheson purity ethylene from Matheson Gas. X-ray measurements were made with a Bruker DUO platform diffractometer equipped with a 4K CCD APEX II detector and an Incoatec 30 W Cu microsource with compact multilayer optics. Data were collected using a narrow-frame algorithm with scan widths of 0.5° in ω and an exposure time of 25 s/frame at 123 K. The data were integrated using the Bruker-Nonius SAINT program, with the intensities corrected for Lorentz factor, polarization, air absorption, and absorption due to variation in the path length through the detector faceplate. The data were scaled, and an absorption correction was applied using SADABS. Redundant reflections were averaged. The structure was solved by using the program SHELXT and refined using SHELXL. DSC measurements were collected on a TA Instruments DSC2500 system using a heat-cool-heat method with a nitrogen flow of 80 mL/min. The sample was heated at 10 °C/min from 25 to 200 °C then cooled from 200 °C to -90 °C at 5 °C/min. The sample was then heated from -90 to 200 °C at 10 °C/min. All reported melting temperatures come from

the second heating cycle. GPC analysis was performed on a Malvern Viscotec 350A HT-GPC System using triple detection (a refractive index detector, a viscometer, and a light scattering detector) and a polystyrene standard to determine the molecular weight. Three TSKgel GHMHR-H(S)HT mixed-bed columns were used with a 1,2,4-trichlorobenzene flow of 1.0 mL/min at 160 °C. All samples were dissolved in 1,2,4-trichlorobenzene at 160 °C. Samples were heated for at least 2 h to dissolve.

General Procedure for Polymerizations Using Nickel Precatalysts. A 450 mL Parr reactor with a mechanical stirrer was heated at 100 °C for at least 2 h under vacuum. After it was cooled to room temperature, the reactor was pressurized to the desired pressure of ethylene followed by venting. Toluene (150 mL, unless otherwise indicated) was added via syringe, and the reactor was sealed. The reactor was pressurized to ca. 13.6 atm and the temperature was allowed to reach the desired value. After the temperature reached the desired value, the reactor was vented. A solution of MMAO-3A (7 wt % Al in heptane, 0.5 mmol, 0.27 mL) was rapidly added. A stock solution of the catalyst was prepared by dissolving the catalyst (5 μ mol) in chlorobenzene (5 mL). An appropriate amount of stock solution was then diluted by toluene (2 mL) and quickly added to the reaction mixture. After that the reactor was sealed and pressurized to the desired ethylene pressure with fast stirring. The exotherm of the polymerization was controlled, and the temperature was maintained using an ice/water bath. The reaction mixture was stirred for the appropriate time. After that, the reactor was vented and the polymer and remaining liquid were stirred with a 1/1 10% aqueous HCl/90% MeOH solution (100 mL) followed by filtration. The polymer was washed with methanol and acetone and dried overnight in a vacuum oven at 60 °C.

General Procedure for Polymerizations Using Palladium Catalysts. A 450 mL Parr reactor with a mechanical stirrer was heated at 100 °C for at least 2 h under vacuum. After it was cooled to room temperature, the reactor was pressurized to the desired pressure of ethylene followed by venting. Methylene chloride (50 mL, unless otherwise indicated) was added via syringe, and the reactor was sealed. The reactor was pressurized to ca. 13.6 atm, and the temperature was allowed to reach the desired value. After the temperature reached the desired value, the reactor was vented. A freshly prepared solution (10 μ mol in 2.0 mL of CH₂Cl₂) of catalyst was rapidly added. After that the reactor was sealed and pressurized to the desired ethylene pressure with fast stirring. The reaction mixture was stirred for the appropriate time. After that, the reactor was vented and a 1/1 10% aqueous HCl/90% MeOH solution (2 mL) was added, followed by filtration through a pad of silica gel into a round-bottom flask. After removal of the volatiles by rotary evaporation, the residue was dissolved in hexanes and filtered through a pad of silica gel. The solvent was evaporated, affording the product as a colorless liquid.

General Procedure for Variable-Temperature NMR Experiments. Inside a glovebox, a fresh solution of **14a-syn** (8.3 mg, 12 μ mol) in tetrachloroethane-*d*₂ (0.6 mL) was placed in a screw-capped NMR tube. The tube was capped, wrapped with Parafilm, and removed from the glovebox. The tube was then transferred to a NMR probe for data acquisition. The sample was allowed to equilibrate for at least 5 min at the indicated probe temperature prior to each measurement. The isomerization of **14a** exhibits reversible first-order kinetics and was monitored by following the integration of signals at 10.00–9.89 ppm (**14a-syn**) and at 9.77–9.74 ppm (**14a-anti**). At equilibrium, the *syn/anti* isomer ratio is ca. 1.2/1.

2,3-Dihydrophenanthren-4(1H)-one (7a). This compound was synthesized using a modified literature procedure.^{36–38} A 500 mL three-necked round-bottom flask equipped with a magnetic stir bar was charged with CH₂Cl₂ (100 mL), nitromethane (500 mL), succinic anhydride (8.2 g, 64 mmol), and AlCl₃ (25.6 g, 192 mmol). The flask was immersed in an ice bath, and a solution of naphthalene (5.8 g, 58 mmol) in CH₂Cl₂ (40 mL) was added dropwise to the stirred mixture over a 1 h period. After 30 min, the ice bath was removed and the dark solution was stirred overnight. The reaction mixture was carefully poured into a mixture of ice and concentrated HCl. Hexanes (200 mL) was added, and the mixture was stirred for

10 min. The precipitate was collected by filtration and was thoroughly washed with H₂O. The solid was recrystallized from acetic acid to afford purple crystals of 4-(naphthalen-2-yl)-4-oxobutanoic acid (8.1 g, 55%). To a solution of the keto acid (7.3 g, 32 mmol) in diethylene glycol (200 mL) was added hydrazine monohydrate (5.7 g, 113 mmol), and the reaction mixture was stirred at 100 °C for 1 h. KOH (6.2 g, 110 mmol) was added, and the reaction mixture was stirred at 260 °C for 2 h. After the mixture was cooled to room temperature, H₂O (100 mL) was added, and the mixture was poured into a mixture of ice and concentrated HCl. The precipitate was removed by filtration and was thoroughly washed with H₂O. The crude product was dissolved in CH₂Cl₂ (400 mL) and washed with H₂O (2 \times 100 mL). The organic phase was dried over anhydrous MgSO₄ and filtered. The solvent was evaporated, affording the product as greenish yellow solid of 4-(naphthalen-2-yl)butanoic acid (5.8 g, 85%). A 250 mL round-bottom flask equipped with a magnetic stir bar was charged with the acid (5.6 g, 26 mmol) and methanesulfonic acid (40 mL). The solution was stirred for 1 h at 95 °C. After it was cooled to room temperature, the reaction mixture was poured into ice and extracted with Et₂O (3 \times 100 mL). The combined organic phases were washed with saturated aqueous NaHCO₃ (2 \times 100 mL) and were dried over anhydrous MgSO₄. The solvent was evaporated, affording the product as yellow solid (4.7 g, 92%). This compound is known.³⁷ ¹H NMR (600 MHz, CDCl₃, ppm): δ 9.43 (d, *J* = 8.4 Hz, 1H), 7.90 (d, *J* = 8.4 Hz, 1H), 7.80 (d, *J* = 8.4 Hz, 1H), 7.67–7.58 (m, 1H), 7.49 (dd, *J* = 7.3, 7.3 Hz, 1H), 7.29 (d, *J* = 8.4 Hz, 1H), 3.09 (t, *J* = 6.1 Hz, 2H), 2.78 (dd, *J* = 7.3, 6.0 Hz, 2H), 2.23–2.12 (m, 3H). ¹³C NMR (151 MHz, CDCl₃, ppm): δ 200.6, 146.9, 134.3, 132.8, 131.4, 128.9, 128.4, 127.3, 127.1, 126.7, 125.9, 41.2, 31.6, 23.1.

6,7-Dimethyl-2,3-dihydrophenanthren-4(1H)-one (7b). This compound was synthesized using a modified literature procedure.^{36–38} A 500 mL three-necked round-bottom flask equipped with a magnetic stir bar was charged with CH₂Cl₂ (30 mL), nitromethane (25 mL), succinic anhydride (2.9 g, 29 mmol), and AlCl₃ (12.8 g, 96 mmol). The flask was immersed in an ice bath, and a solution of 2,3-dimethylnaphthalene (5.0 g, 32 mmol) in CH₂Cl₂ (40 mL) was added dropwise to the stirred mixture over a 1 h period. After 30 min, the ice bath was removed and the dark solution was stirred overnight. The reaction mixture was carefully poured into a mixture of ice and concentrated HCl. Hexanes (200 mL) was added, and the mixture was stirred for 10 min. The precipitate was collected by filtration and was thoroughly washed with H₂O. The solid was recrystallized from acetic acid to afford purple crystals of 4-(6,7-dimethylnaphthalen-2-yl)-4-oxobutanoic acid (5.9 g, 72%). To a solution of the keto acid (5.1 g, 20 mmol) in diethylene glycol (150 mL) was added hydrazine monohydrate (3.5 g, 70 mmol), and the reaction mixture was stirred at 100 °C for 1 h. Potassium hydroxide (3.9 g, 70 mmol) was added, and the reaction mixture was stirred at 260 °C for 2 h. After the mixture was cooled to room temperature, H₂O (50 mL) was added, and the mixture was poured into a mixture of ice and concentrated HCl. The precipitate was removed by filtration and was thoroughly washed with H₂O. The crude product was dissolved in CH₂Cl₂ (400 mL), and the solution was washed with H₂O (2 \times 100 mL). The organic phase was dried over anhydrous MgSO₄ and filtered. The solvent was evaporated, affording the product as greenish yellow solid of 4-(6,7-dimethylnaphthalen-2-yl)butanoic acid (4.0 g, 83%). A 250 mL round-bottom flask equipped with a magnetic stir bar was charged with the acid (4.0 g, 16.5 mmol) and methanesulfonic acid (60 mL). The solution was stirred for 2 h at 50 °C. After it was cooled to room temperature, the reaction mixture was poured into ice and extracted with Et₂O (3 \times 100 mL). The combined organic phases were washed with saturated aqueous NaHCO₃ (2 \times 100 mL) and were dried over anhydrous MgSO₄. The solvent was evaporated, affording the product as a yellow solid (2.9 g, 77%). This compound is known.³⁶ ¹H NMR (400 MHz, CDCl₃, ppm): δ 9.20 (s, 1H), 7.81 (d, *J* = 8.4 Hz, 1H), 7.54 (s, 1H), 7.22 (d, *J* = 8.4 Hz, 1H), 3.09 (t, *J* = 6.1 Hz, 2H), 2.77 (t, *J* = 6.6 Hz, 2H), 2.47 (s, 3H), 2.41 (s, 3H), 2.24–2.10 (m, 2H). ¹³C NMR (151 MHz, CDCl₃, ppm): δ 200.7, 146.0, 139.0, 135.4, 133.5, 131.9, 130.2, 128.0, 126.7, 126.3, 126.1, 41.2, 31.7, 23.2, 20.9, 20.0.

2,3-Dihydrophenanthren-4(1H)-one O-Pivaloyl Oxime (8a).

A 100 mL round-bottom flask equipped with a magnetic stir bar and a condenser was charged with **7a** (4.7 g, 24 mmol), $\text{NH}_2\text{OH}\cdot\text{HCl}$ (2.7 g, 39 mmol), NaOH (5.1 g, 128 mmol), EtOH (60 mL), and H_2O (6 mL). The reaction mixture was stirred at reflux for 30 min. After it was cooled to room temperature, the reaction mixture was poured into H_2O (200 mL). The precipitate was collected by filtration and thoroughly washed with H_2O , affording the 2,3-dihydrophenanthren-4(1H)-one oxime as a white solid (5.0 g, 99%). A 100 mL round-bottom flask equipped with a magnetic stir bar was charged with the oxime (2.1 g, 10 mmol) and CH_2Cl_2 (150 mL). The flask was immersed in an ice bath, and Et_3N (4.2 mL, 30 mL) was added, followed by pivaloyl chloride (2.6 mL, 20 mmol). The ice bath was removed, and the reaction mixture was stirred at room temperature overnight. The reaction mixture was transferred to a separatory funnel. The organic phase was washed with H_2O (3 \times 100 mL). The combined organic phases were dried over anhydrous MgSO_4 , filtered, concentrated on silica gel, and purified by column chromatography on silica gel (eluent hexanes/ EtOAc 6/1), affording the product as a light yellow solid (2.9 g, 94%). $^1\text{H NMR}$ (600 MHz, CDCl_3 , ppm): δ 9.27 (d, J = 8.3 Hz, 1H), 7.80 (d, J = 8.3 Hz, 2H), 7.67–7.57 (m, 1H), 7.46 (dd, J = 7.2, 7.1 Hz, 1H), 7.28 (d, J = 8.3 Hz, 1H), 3.04 (t, J = 6.8 Hz, 2H), 2.92–2.85 (m, 2H), 1.94–1.83 (m, 2H), 1.39 (s, 9H). $^{13}\text{C NMR}$ (151 MHz, CDCl_3 , ppm): δ 175.3, 163.2, 142.3, 133.4, 131.2, 130.9, 128.4, 128.2, 127.6, 126.7, 125.6, 125.3, 39.0, 31.3, 27.5, 27.0, 20.9. HRMS (+ESI): calculated for $\text{C}_{19}\text{H}_{21}\text{NO}_2$ [$\text{M} + \text{Na}$] $^+$ 318.1465, found 318.1466.

6,7-Dimethyl-2,3-dihydrophenanthren-4(1H)-one O-Pivaloyl Oxime (8b). A 100 mL round-bottom flask equipped with a magnetic stir bar and a condenser was charged with **7b** (2.85 g, 12.7 mmol), $\text{NH}_2\text{OH}\cdot\text{HCl}$ (1.41 g, 20.3 mmol), NaOH (2.54 g, 63.5 mmol), EtOH (15 mL), and H_2O (3 mL). The reaction mixture was stirred at reflux for 30 min. After it was cooled to room temperature, the reaction mixture was poured into H_2O (100 mL). The precipitate was collected by filtration and thoroughly washed with H_2O , affording the 6,7-dimethyl-2,3-dihydrophenanthren-4(1H)-one oxime as a white solid (3.0 g, 99%). A 100 mL round-bottom flask equipped with a magnetic stir bar was charged with the oxime (1.2 g, 5 mmol) and CH_2Cl_2 (80 mL). The flask was immersed in an ice bath, and Et_3N (2.1 mL, 15 mL) was added, followed by pivaloyl chloride (1.3 mL, 10 mmol). The ice bath was removed, and the reaction mixture was stirred at room temperature overnight. The reaction mixture was transferred to a separatory funnel. The organic phase was washed with H_2O (3 \times 50 mL). The combined organic phases were dried over anhydrous MgSO_4 , filtered, concentrated on silica gel and purified by column chromatography on silica gel (eluent hexanes/ EtOAc 6/1), affording the product as a white solid (1.5 g, 90%). $^1\text{H NMR}$ (400 MHz, CDCl_3 , ppm): δ 9.10 (s, 1H), 7.69 (d, J = 8.3 Hz, 1H), 7.54 (s, 1H), 7.18 (d, J = 8.3 Hz, 1H), 3.02 (t, J = 6.8 Hz, 2H), 2.86 (t, J = 6.0 Hz, 2H), 2.50 (s, 3H), 2.41 (s, 3H), 1.93–1.81 (m, 2H), 1.40 (s, 9H). $^{13}\text{C NMR}$ (101 MHz, CDCl_3 , ppm): δ 175.3, 163.3, 141.4, 138.0, 135.1, 132.3, 130.3, 129.7, 127.9, 127.4, 125.8, 124.3, 39.0, 31.3, 27.6, 27.0, 21.2, 21.0, 20.0. HRMS (+ESI): calculated for $\text{C}_{21}\text{H}_{25}\text{NO}_2$ [$\text{M} + \text{Na}$] $^+$ 346.1778, found 346.1779.

Phenanthren-4-amine (9a). This compound was synthesized using a modified literature procedure.³⁹ A 150 mL pressure vessel equipped with a magnetic stir bar was charged with **8a** (1.48 g, 5 mmol), $\text{Pd}(\text{OAc})_2$ (0.12 g, 0.5 mmol), and pivalic acid (0.16 g, 1.5 mmol). The vessel was flushed with nitrogen, capped, and placed inside a glovebox. To this mixture were added K_2CO_3 (2.8 g, 20 mmol), toluene (35 mL), and tricyclopentylphosphine (0.25 mL, 1 mmol). The vessel was capped, taken out of the glovebox, stirred at room temperature for 5 min, and placed in a preheated oil bath (110 $^\circ\text{C}$) for 3 days. After it was cooled to room temperature, the reaction mixture was filtered through a pad of neutral alumina. The solids were washed with EtOAc (200 mL). The combined filtrate and washings were concentrated on silica gel and purified by column chromatography on silica gel (eluent hexanes/ EtOAc 10/1), affording **9a** as a tan solid (0.49 g, 51%). This compound is known.⁴⁰ $^1\text{H NMR}$ (600 MHz, CDCl_3 , ppm): δ 9.26 (d, J = 8.4 Hz, 1H), 7.91 (d, J = 7.7 Hz, 1H),

7.72–7.55 (m, 4H), 7.47–7.36 (m, 2H), 7.01 (dd, J = 6.6, 2.2 Hz, 1H), 4.42 (s, 2H). $^{13}\text{C NMR}$ (151 MHz, CDCl_3 , ppm): δ 145.2, 134.5, 132.9, 131.0, 128.8, 127.9, 127.3, 126.8, 126.1, 125.8, 125.6, 120.3, 119.7, 115.6. HRMS (+ESI): calculated for $\text{C}_{14}\text{H}_{11}\text{N}$ [$\text{M} + \text{H}$] $^+$ 194.0964, found 194.0962.

6,7-Dimethylphenanthren-4-amine (9b). This compound was synthesized using the procedure described for **9a** with oxime **8b** (1.62 g, 5 mmol), $\text{Pd}(\text{OAc})_2$ (0.12 g, 0.5 mmol), tricyclopentylphosphine (0.25 mL, 1.0 mmol), pivalic acid (0.16 g, 1.5 mmol), K_2CO_3 (2.8 g, 20 mmol), and toluene (35 mL). Yield: 0.93 g, 84%. $^1\text{H NMR}$ (400 MHz, CDCl_3 , ppm): δ 8.99 (s, 1H), 7.65 (s, 1H), 7.57 (s, 2H), 7.37–7.32 (m, 2H), 7.01–6.94 (m, 1H), 4.42 (s, 2H), 2.51 (s, 3H), 2.46 (s, 3H). $^{13}\text{C NMR}$ (101 MHz, CDCl_3 , ppm): δ 145.0, 135.2, 134.8, 134.3, 131.5, 129.3, 129.0, 126.9, 126.8, 126.3, 126.1, 120.3, 119.6, 115.2, 20.9, 19.9. HRMS (+ESI): calculated for $\text{C}_{16}\text{H}_{15}\text{N}$ [$\text{M} + \text{H}$] $^+$ 222.1277, found 222.1275.

Ligand 10a. This compound was synthesized using a modified literature procedure.⁴¹ A 2 dram vial was charged with **9a** (235 mg, 1.2 mmol), 2,3-butadione (52 mg, 0.6 mmol), formic acid (2 drops), and methanol (2 mL). The reaction mixture was stirred at 80 $^\circ\text{C}$ overnight. A yellow precipitate formed. After the mixture was cooled to room temperature, the solid was collected by filtration, washed with cold methanol, and dried under vacuum, affording the product as a yellow solid (233 mg, 89%). $^1\text{H NMR}$ (600 MHz, CDCl_3 , ppm): δ 9.07 (d, J = 8.5 Hz, 2H), 7.93 (d, J = 7.5 Hz, 2H), 7.84–7.71 (m, 6H), 7.64 (dd, J = 7.6, 7.6 Hz, 2H), 7.58 (dd, J = 7.0, 7.3 Hz, 2H), 7.48 (dd, J = 7.3, 7.2 Hz, 2H), 6.96 (d, J = 7.3 Hz, 2H), 2.43 (s, 6H). $^{13}\text{C NMR}$ (151 MHz, CDCl_3 , ppm): δ 167.9, 149.2, 134.4, 133.3, 130.8, 128.7, 128.1, 127.9, 127.7, 126.5, 126.4, 126.1, 125.5, 121.7, 116.7, 16.8. HRMS (+ESI): calculated for $\text{C}_{32}\text{H}_{24}\text{N}_2$ [$\text{M} + \text{H}$] $^+$ 437.2012, found 437.2012.

Ligand 10b. This compound was synthesized using the procedure described for ligand **10a** with amine **9b** (332 mg, 1.5 mmol), 2,3-butadione (60 mg, 0.7 mmol), HCOOH (2 drops), and methanol (5 mL). Yield: 0.29 g, 83%. $^1\text{H NMR}$ (400 MHz, CD_2Cl_2 , ppm): δ 8.82 (s, 2H), 7.91–7.36 (m, 10H), 6.92 (d, J = 7.5 Hz, 2H), 2.41 (s, 12H), 2.09 (s, 6H). $^{13}\text{C NMR}$ (101 MHz, CD_2Cl_2 , ppm): δ 168.1, 149.6, 136.0, 135.8, 134.6, 132.2, 129.0, 128.9, 127.7, 127.0, 126.4, 125.6, 121.6, 116.6, 31.2, 20.8, 20.0, 16.6. HRMS (+ESI): calculated for $\text{C}_{36}\text{H}_{32}\text{N}_2$ [$\text{M} + \text{H}$] $^+$ 493.2638, found 493.2639.

Ligand 11a. This compound was synthesized using a modified literature procedure.^{22,29} A 2 dram vial was charged with **9a** (440 mg, 2.3 mmol), acenaphthenequinone (200 mg, 1.1 mmol), ZnCl_2 (180 mg, 1.3 mmol), and acetic acid (4 mL). The reaction mixture was stirred at 120 $^\circ\text{C}$ for 30 min. After the mixture was cooled to room temperature, the solid was separated by filtration, washed with acetic acid, and dried under vacuum, affording the zinc complex as a dark red solid. A 100 mL round-bottom flask equipped with a magnetic stir bar was charged with the zinc complex, sodium oxalate (1.34 g, 10 mmol), methylene chloride (10 mL), and H_2O (2 mL). The reaction mixture was stirred at room temperature for 1 h. The two phases were separated, the organic layer was dried over anhydrous Na_2SO_4 and filtered, and the solvents were evaporated, affording the product as a red solid (0.58 g, 98%). The $^1\text{H NMR}$ spectrum shows two isomers in a ca. 7:1 ratio in CD_2Cl_2 at room temperature. $^1\text{H NMR}$ (600 MHz, CD_2Cl_2 , ppm): major isomer, δ 9.81–9.49 (m, 2H), 7.96–7.88 (m, 6H), 7.84 (d, J = 8.8 Hz, 2H), 7.77 (d, J = 8.2 Hz, 2H), 7.71 (dd, J = 7.6, 7.8 Hz, 2H), 7.67–7.61 (m, 2H), 7.59–7.53 (m, 2H), 7.40 (d, J = 7.3, 2H), 7.19 (dd, J = 7.8, 7.8 Hz, 2H), 6.53 (d, J = 7.5 Hz, 2H); minor isomer, δ 9.33 (d, J = 8.5 Hz, 2H), 8.44 (d, J = 7.0 Hz, 2H), 8.07 (d, J = 8.3 Hz, 2H), 7.46 (t, J = 7.7, 7.7 Hz, 2H), 7.12 (dd, J = 7.7, 7.9 Hz, 2H), 7.06 (dd, J = 6.9, 7.4 Hz, 2H), 6.88 (d, J = 6.5 Hz, 2H), 6.20 (d, J = 7.2 Hz, 2H). Signals of 10 protons of the minor isomer could not be located due to overlap with the major isomer. $^{13}\text{C NMR}$ (151 MHz, CD_2Cl_2 , ppm): major isomer, δ 151.0, 142.1, 135.1, 133.7, 131.7, 131.2, 129.6, 129.5, 129.4, 128.9, 128.5, 128.1, 128.0, 127.4, 126.6, 126.4, 126.1, 124.0, 122.2, 116.8, 116.6. Signals of carbons of the minor isomer are not listed due to their low intensity. HRMS (+ESI): calculated for $\text{C}_{40}\text{H}_{24}\text{N}_2$ [$\text{M} + \text{H}$] $^+$ 533.2012, found 533.2010.

Ligand 11b. This compound was synthesized using the procedure described for ligand 11a with amine **9b** (0.48 g, 2.2 mmol), acenaphthenequinone (0.18 g, 1 mmol), ZnCl₂ (0.16 g, 1.2 mmol), acetic acid (5 mL), sodium oxalate (1.34 g, 10 mmol), CH₂Cl₂ (20 mL), and H₂O (10 mL). Yield: 0.53 g, 90%. ¹H NMR (600 MHz, CD₂Cl₂, ppm): δ 9.35 (s, 2H), 7.90 (dd, *J* = 7.8, 1.3 Hz, 2H), 7.81 (d, *J* = 8.8 Hz, 2H), 7.76 (dd, *J* = 8.2, 8.8 Hz, 4H), 7.68 (dd, *J* = 7.6, 7.6 Hz, 2H), 7.65 (s, 2H), 7.32 (dd, *J* = 7.4, 1.3 Hz, 2H), 7.19 (dd, *J* = 7.6, 8.2 Hz, 2H), 6.49 (d, *J* = 7.4 Hz, 2H), 2.46 (s, 6H), 2.40 (s, 6H). ¹³C NMR (151 MHz, CD₂Cl₂, ppm): δ 160.9, 151.3, 142.6, 136.8, 136.4, 135.3, 132.7, 132.0, 130.9, 129.7, 129.64, 129.62, 129.3, 128.5, 128.4, 127.2, 127.1, 126.4, 124.3, 122.3, 115.8, 21.8, 20.4. HRMS (+ESI): calculated for C₄₄H₃₂N₂ [M + H]⁺ 589.2638, found 589.2639.

Palladium Complex 12a. Ligand **10a** (120 mg, 0.275 mmol) and Pd(COD)MeCl (67 mg, 0.25 mmol) were placed in a 50 mL Schlenk flask equipped with a magnetic stir bar. Methylene chloride (10 mL) was added, and the reaction mixture was stirred at room temperature overnight. Pentane (20 mL) was added, and the solid was collected by filtration, washed with pentane (2 × 10 mL), and dried under vacuum, affording the product as an orange solid (110 mg, 74%). The ¹H NMR spectrum shows two isomers in a ca. 1.5/1 ratio in CD₂Cl₂ at room temperature. ¹H NMR (600 MHz, CD₂Cl₂, ppm): δ 9.54 (d, *J* = 8.4 Hz, 1H, minor), 9.41 (d, *J* = 8.5 Hz, 1H, minor), 9.22 (d, *J* = 8.5 Hz, 1H, major), 9.16 (d, *J* = 8.5 Hz, 1H, major), 8.07–7.64 (m, major and minor signals overlap), 7.38 (dd, *J* = 7.5, 1.4 Hz, 1H, major), 7.36 (dd, *J* = 7.4, 1.3 Hz, 1H, major), 7.32 (dd, *J* = 4.2, 1.4 Hz, 1H, minor), 7.31 (dd, *J* = 4.2, 1.4 Hz, 1H, minor), 1.86 (s, 3H, minor), 1.84 (s, 3H, major), 1.83 (s, 3H, minor), 1.78 (s, 3H, major), 0.49 (s, 3H, major), 0.47 (s, 3H, minor). ¹³C NMR measurements were not taken due to the poor solubility of the compound. HRMS (+ESI): calculated for C₃₃H₂₇N₂Pd [M]⁺ 557.1216, found 557.1214.

Palladium Complex 13a. Complex **12a** (89 mg, 0.15 mmol), NaBARf (140 mg, 0.15 mmol), and acetonitrile (0.1 mL) were placed in a 50 mL Schlenk flask equipped with a magnetic stir bar. Methylene chloride (30 mL) was added, and the reaction mixture was stirred at room temperature for 4 h. The mixture was filtered through a pad of Celite, and the volatiles were removed. The residue was washed with pentane (2 × 10 mL) and dried under vacuum, affording the product as a red solid (190 mg, 87%). The ¹H NMR spectrum shows two isomers in a ca. 1/1 ratio in CD₂Cl₂ at room temperature. ¹H NMR (600 MHz, CD₂Cl₂, ppm): δ 9.19 (d, *J* = 8.5 Hz, 1H), 9.09 (d, *J* = 8.4 Hz, 1H), 8.87 (d, *J* = 8.3 Hz, 1H), 8.83 (d, *J* = 8.4 Hz, 1H), 8.13–7.99 (m, *syn* and *anti* signals overlap), 7.97–7.88 (m, *syn* and *anti* signals overlap), 7.87–7.70 (m, *syn* and *anti* signals overlap), 7.55 (s, 8H), 7.32–7.169 (m, *syn* and *anti* signals overlap), 2.492 (s, 3H), 2.490 (s, 3H), 2.13 (s, 3H), 2.09 (s, 3H), 1.28 (s, 3H), 1.25 (s, 3H), 0.402 (s, 3H), 0.400 (s, 3H). ¹³C NMR (151 MHz, CD₂Cl₂, ppm): δ 181.4, 181.2, 172.3, 171.8, 162.3 (q, *J*_{C–B} = 50 Hz), 144.1, 144.0, 143.8, 143.6, 135.3 (bs), 135.0, 134.9, 134.8, 134.5, 134.4, 134.0, 133.9, 130.5, 130.4, 130.15, 130.13, 130.09, 130.06, 130.0, 129.7, 129.6, 129.5, 129.44, 129.38 (q, *J*_{C–F} = 32 Hz), 129.3, 129.1, 128.9, 128.7, 128.29, 128.27, 128.2, 128.04, 127.99, 127.96, 127.9, 127.80, 127.78, 127.6, 127.5, 127.4, 127.22, 127.20, 127.1, 126.9, 126.6, 125.1 (q, *J*_{C–F} = 273 Hz), 123.5, 123.4, 123.0, 122.9, 121.7, 121.29, 121.26, 121.1, 121.0, 120.5, 118.1–117.9 (m), 22.4, 22.0, 21.6, 21.1, 7.1, 7.0, 2.3, 2.2. The signals of five carbons could not be located. ¹⁹F NMR (565 MHz, CD₂Cl₂, ppm): δ –62.7. HRMS (+ESI): calculated for C₃₃H₃₀N₃Pd [M]⁺ 598.1482, found 598.1475.

Palladium Complex 14a. This complex was synthesized using the procedure described for complex **12a** with ligand **11a** (150 mg, 0.275 mmol), Pd(COD)MeCl (70 mg, 0.25 mmol), and CH₂Cl₂ (50 mL). Yield: 120 mg, 70%. The ¹H NMR spectrum shows two isomers in a ca. 1/1 ratio in CD₂Cl₂ at room temperature. X-ray-quality crystals were grown by layering pentane over a solution of **14a** in CH₂Cl₂ at room temperature. The *syn* and *anti* isomers crystallize concurrently, and crystal picking allowed us to obtain each isomer for X-ray analysis. ¹H NMR (600 MHz, CD₂Cl₂, ppm): δ 9.94 (dd, *J* = 8.2, 8.2 Hz, 2H, *syn*), 9.76 (d, *J* = 8.6 Hz, 1H, *anti*), 9.73 (d, *J* = 8.5 Hz, 1H, *anti*), 8.16 (d, *J* = 7.9 Hz, 1H, *anti*), 8.14 (d, *J* = 7.9 Hz, 1H,

syn), 8.10–8.05 (m, *syn* and *anti* signals overlap), 8.03–7.57 (m, *syn* and *anti* signals overlap), 7.21–7.08 (m, *syn* and *anti* signals overlap), 6.30 (d, *J* = 7.5 Hz, 1H, *syn*), 8.28 (d, *J* = 7.4 Hz, 1H, *anti*), 6.07 (d, *J* = 7.5 Hz, 1H, *syn*), 6.03 (d, *J* = 7.6 Hz, 1H, *anti*), 0.79 (s, 3H, *anti*), 0.75 (s, 3H, *syn*). ¹³C NMR (151 MHz, CD₂Cl₂, ppm): δ 173.4, 173.1, 168.5, 168.3, 145.8, 145.7, 145.4, 145.2, 144.73, 144.68, 135.0, 134.9, 134.7, 134.6, 134.2, 134.1, 134.0, 133.9, 131.84, 131.81, 131.52, 131.50, 131.40, 131.36, 130.0, 129.8, 129.7, 129.63, 129.60, 129.5, 129.38, 129.35, 129.3, 129.21, 129.18, 129.16, 129.11, 129.08, 129.02, 128.98, 128.87, 128.85, 128.8, 128.7, 128.5, 128.00, 127.96, 127.9, 127.77, 127.75, 127.7, 127.62, 127.55, 127.4, 127.29, 127.26, 127.22, 127.21, 127.16, 127.0, 126.6, 126.5, 125.4, 125.3, 125.19, 125.15, 123.8, 123.7, 123.6, 123.5, 122.6, 122.2, 121.1, 120.6, 3.2, 3.1. The signals of six carbons could not be located. HRMS (+ESI): calculated for C₄₁H₂₇N₂Pd [M]⁺ 653.1218, found 653.1199.

Palladium Complex 14a-syn. Ligand **11a** (150 mg, 0.275 mmol) and Pd(COD)MeCl (67 mg, 0.25 mmol) were placed in a 500 mL Schlenk flask equipped with a magnetic stir bar. Methylene chloride (50 mL) was added, and the reaction mixture was stirred at room temperature overnight. A small sample was taken and characterized by ¹H NMR, showing a ca. 1/1 mixture of *syn/anti* isomers. Toluene (250 mL) was added, and the resulting mixture was carefully concentrated at 60 °C until ca. 100 mL. The solid was collected by filtration, washed with toluene (10 mL), and dried under vacuum, affording the product as red solid (93 mg, 54%). The ¹H NMR spectrum shows nearly pure **14a-syn** with a *syn/anti* isomer ratio of ca. 30/1. The filtrate was brought to dryness at 60 °C. The residue was dissolved in CD₂Cl₂ and characterized by ¹H NMR, showing a ca. 3/1 mixture of *syn/anti* isomers. X-ray-quality crystals were grown by layering pentane over a solution of **12b-syn** in CH₂Cl₂ at –20 °C. ¹H NMR (600 MHz, CD₂Cl₂, ppm): δ 9.95 (dd, *J* = 8.5, 8.5 Hz, 2H), 8.14 (d, *J* = 7.6 Hz, 1H), 8.06 (d, *J* = 7.7 Hz, 1H), 8.03–7.82 (m, 11H), 7.80 (dd, *J* = 7.6, 7.6 Hz, 1H), 7.75–7.55 (m, 4H), 7.18 (dd, *J* = 7.9, 7.9 Hz, 1H), 7.14 (dd, *J* = 7.9, 7.9 Hz, 1H), 6.30 (d, *J* = 7.5 Hz, 1H), 6.07 (d, *J* = 7.5 Hz, 1H), 0.75 (s, 3H). ¹³C NMR (151 MHz, CD₂Cl₂, ppm): δ 173.2, 168.3, 145.6, 145.0, 144.5, 134.5, 134.3, 133.8, 133.6, 131.7, 131.2, 131.1, 129.7, 129.48, 129.46, 129.2, 128.1, 129.01, 128.95, 128.9, 128.7, 128.6, 128.2, 127.83, 127.77, 127.61, 127.56, 127.4, 127.12, 127.07, 127.0, 126.2, 125.2, 125.1, 123.3, 122.3, 120.8, 3.0. The signals of three carbons could not be located. HRMS (+ESI): calculated for C₄₁H₂₇N₂Pd [M]⁺ 653.1218, found 653.1214.

Palladium Complex 14b. This complex was synthesized using the procedure described for complex **12a** with ligand **11b** (130 mg, 0.22 mmol), Pd(COD)MeCl (54 mg, 0.20 mmol), and CH₂Cl₂ (10 mL). Yield: 120 mg, 80%. X-ray-quality crystals were grown by layering pentane over a solution of **14b** in CH₂Cl₂ at room temperature. ¹H NMR (600 MHz, CD₂Cl₂, ppm): δ 9.81 (s, 1H), 9.80 (s, 1H), 8.11 (dd, *J* = 7.9, 1.4 Hz, 1H), 8.03 (dd, *J* = 7.9, 1.3 Hz, 1H), 7.91–7.77 (m, 7H), 7.74 (d, *J* = 8.8 Hz, 1H), 7.67 (s, 1H), 7.63 (s, 1H), 7.56 (dd, *J* = 7.4, 1.4 Hz, 1H), 7.53 (dd, *J* = 7.4, 1.3 Hz, 1H), 7.14 (dd, *J* = 7.9, 7.9 Hz, 1H), 7.11 (dd, *J* = 7.9, 7.9 Hz, 1H), 6.15 (d, *J* = 7.4 Hz, 1H), 5.96 (d, *J* = 7.4 Hz, 1H), 2.69 (s, 3H), 2.67 (s, 3H), 2.41 (s, 3H), 2.40 (s, 3H), 0.82 (s, 3H). ¹³C NMR (151 MHz, CD₂Cl₂, ppm): δ 172.9, 168.1, 145.6, 145.0, 144.8, 137.3, 136.9, 136.8, 136.3, 134.9, 134.6, 132.7, 132.5, 131.7, 131.5, 131.3, 130.0, 129.7, 129.6, 129.4, 129.3, 129.2, 129.1, 128.9, 128.6, 128.4, 127.8, 127.4, 127.3, 127.0, 126.8, 126.7, 126.5, 125.2, 125.1, 123.4, 123.2, 121.3, 119.8, 21.74, 21.66, 20.03, 20.01, 3.1. The signal of one carbon could not be located. HRMS (+ESI): calculated for C₄₅H₃₅N₂Pd [M]⁺ 709.1846, found 709.1847.

Palladium Complex 15a. This complex was synthesized using the procedure described for complex **13a** with complex **14a** (120 mg, 0.17 mmol), NaBARf (160 mg, 0.17 mmol), acetonitrile (0.2 mL), and CH₂Cl₂ (20 mL). Yield: 230 mg, 89%. The ¹H NMR spectrum shows two isomers in a ca. 1/1 ratio in CD₂Cl₂ at room temperature. ¹H NMR (600 MHz, CD₂Cl₂, ppm): δ 9.59 (d, *J* = 8.6 Hz, 1H, *syn*), 9.50 (d, *J* = 9.2 Hz, 1H, *syn*), 9.40 (d, *J* = 8.6 Hz, 1H, *anti*), 9.27 (d, *J* = 8.5 Hz, 1H, *anti*), 8.27–8.15 (m, *syn* and *anti* signals overlap), 8.14–8.04 (m, *syn* and *anti* signals overlap), 8.03–7.71 (m, *syn* and *anti* signals overlap), 7.67–7.46 (m, *syn* and *anti* signals overlap),

7.36–7.26 (m, *syn* and *anti* signals overlap), 6.28 (d, $J = 7.5$ Hz, 1H, *syn*), 6.17 (d, $J = 7.5$ Hz, 1H, *anti*), 1.29 (s, 3H, *anti*), 1.28 (s, 3H, *syn*), 0.67 (s, 3H, *anti*), 0.60 (s, 3H, *syn*). ^{13}C NMR (151 MHz, CD_2Cl_2 , ppm): δ 177.4, 177.2, 168.7, 168.4, 162.3 (q, $J_{\text{C}-\text{B}} = 50$ Hz), 146.3, 144.1, 144.1, 144.0, 143.9, 135.1 (bs), 135.2, 135.1, 134.5, 134.4, 134.0, 133.9, 133.6, 133.03, 132.97, 131.9, 131.8, 130.9, 130.7, 130.7, 130.3, 130.2, 130.0, 129.9, 129.8, 129.70, 129.67, 129.6, 129.53, 129.52, 129.41 (q, $J_{\text{C}-\text{F}} = 32$ Hz), 129.40, 129.3, 129.2, 128.9, 128.8, 128.6, 128.4, 128.3, 128.2, 128.10, 128.06, 128.03, 128.01, 127.96, 127.93, 127.89, 127.85, 127.82, 127.80, 127.7, 127.63, 127.57, 126.9, 126.8, 126.5, 126.3, 125.8, 125.7, 125.1 (q, $J_{\text{C}-\text{F}} = 273$ Hz), 123.9, 123.9, 123.5, 123.3, 122.40, 121.8, 121.4, 121.2, 121.2, 120.9, 118.3–117.8 (m), 7.7, 7.6, 2.2 (two Pd-CH₃ signals overlap). Signals of nine carbons could not be located. ^{19}F NMR (565 MHz, CD_2Cl_2 , ppm): δ –62.7. HRMS (+ESI): calculated for $\text{C}_{43}\text{H}_{30}\text{N}_3\text{Pd} [\text{M}]^+$ 694.1484, found 694.1478.

Palladium Complex 15a-syn. Complex 14a-syn (74 mg, 0.11 mmol), NaBARF (100 mg, 0.11 mmol), and acetonitrile (0.05 mL) were placed in a 50 mL Schlenk flask equipped with a magnetic stir bar. Methylene chloride (15 mL) was added, and the reaction mixture was stirred at 0 °C for 4 h. The mixture was filtered through a pad of Celite, and the volatiles were removed under vacuum at 0 °C. The residue was washed with pentane (2 × 10 mL) and dried under vacuum, affording the product as a red solid (140 mg, 86%). The ^1H NMR spectrum shows *syn/anti* isomers in ca. 10/1 ratio in CD_2Cl_2 at room temperature. ^1H NMR (500 MHz, CD_2Cl_2 , ppm): δ 9.60 (d, $J = 8.6$ Hz, 1H), 9.51 (d, $J = 8.4$ Hz, 1H), 8.20 (d, $J = 7.9$ Hz, 1H), 8.16 (dd, $J = 7.5$, 1.3 Hz, 1H), 8.14–8.04 (m, 4H), 8.03–7.95 (m, 4H), 7.89–7.72 (m, 14H), 7.62–7.47 (m, 8H), 7.31 (dd, $J = 7.9$, 8.0 Hz, 1H), 6.29 (d, $J = 7.4$ Hz, 1H), 1.28 (s, 3H), 0.61 (s, 3H). ^{13}C NMR (151 MHz, CD_2Cl_2 , ppm): δ 177.2, 168.2, 162.1 (q, $J_{\text{C}-\text{B}} = 50$ Hz), 146.0, 143.74, 143.72, 135.1 (bs), 134.8, 134.7, 134.1, 133.6, 133.4, 132.8, 131.5, 130.7, 130.5, 130.0, 129.8, 129.5, 129.40, 129.36, 129.2, 129.1 (q, $J_{\text{C}-\text{F}} = 32$ Hz), 129.03, 128.98, 128.9, 128.8, 128.5, 128.2, 128.0, 127.8, 127.7, 127.6, 127.5, 126.7, 126.2, 126.1, 125.6, 124.8 (q, $J_{\text{C}-\text{F}} = 273$ Hz), 123.7, 122.9, 122.2, 121.2, 120.9, 118.1–117.6 (m), 7.2, 2.1. The signal of one carbon could not be located. ^{19}F NMR (565 MHz, CD_2Cl_2 , ppm): δ –62.6. HRMS (+ESI): calculated for $\text{C}_{43}\text{H}_{30}\text{N}_3\text{Pd} [\text{M}]^+$ 694.1484, found 694.1480.

Palladium Complex 15b. This complex was synthesized using the procedure described for complex 13a with complex 14b (120 mg, 0.16 mmol), NaBARF (150 mg, 0.16 mmol), acetonitrile (0.15 mL), and CH_2Cl_2 (10 mL). Yield: 250 mg, 96%. ^1H NMR (600 MHz, CD_2Cl_2 , ppm): δ 9.39 (s, 1H), 9.26 (s, 1H), 8.18 (dd, $J = 8.0$, 1.3 Hz, 1H), 8.15 (dd, $J = 7.9$, 1.3 Hz, 1H), 8.07 (d, $J = 8.0$ Hz, 1H), 8.05 (d, $J = 8.3$ Hz, 1H), 7.92–7.80 (m, 7H), 7.79–7.69 (m, 10H), 7.56 (s, 4H), 7.54–7.43 (m, 3H), 7.29 (dd, $J = 7.9$, 7.9 Hz, 1H), 6.11 (d, $J = 7.5$ Hz, 1H), 2.75 (s, 3H), 2.58 (s, 3H), 2.54 (s, 3H), 2.43 (s, 3H), 1.27 (s, 3H), 0.74 (s, 3H). ^{13}C NMR (151 MHz, CD_2Cl_2 , ppm): δ 177.0, 168.1, 162.4 (q, $J_{\text{C}-\text{B}} = 50$ Hz), 146.4, 143.8, 143.7, 138.2, 137.7, 137.3, 136.9, 135.4 (bs), 135.3, 135.1, 133.6, 133.0, 132.9, 132.6, 131.8, 130.7, 130.5, 130.1, 129.8, 129.6, 129.5 (q, $J_{\text{C}-\text{F}} = 32$ Hz), 129.39, 129.35, 129.3, 129.2, 129.0, 128.1, 127.3, 127.1, 127.04, 127.00, 126.9, 126.8, 126.4, 126.3, 125.7, 125.2 (q, $J_{\text{C}-\text{F}} = 273$ Hz), 123.6, 123.2, 121.3, 121.1, 120.1, 118.3–117.9 (m), 21.80, 21.78, 20.3, 20.0, 7.8, 2.2. ^{19}F NMR (565 MHz, CD_2Cl_2 , ppm): δ –62.5. HRMS (+ESI): calculated for $\text{C}_{47}\text{H}_{38}\text{N}_3\text{Pd} [\text{M}]^+$ 750.2112, found 750.2105.

Nickel Complex 16a. Ligand 10a (120 mg, 0.275 mmol) and (DME)NiBr₂ (74 mg, 0.24 mmol) were placed in a 50 mL Schlenk flask equipped with a magnetic stir bar. Methylene chloride (10 mL) was added, and reaction mixture was stirred at room temperature overnight. Diethyl ether (10 mL) was added, and the solid was collected by filtration, washed with ether (2 × 10 mL), and dried under vacuum, affording the product as a brick red solid (140 mg, 89%). Anal. Calcd for $\text{C}_{32}\text{H}_{24}\text{Br}_2\text{N}_2\text{Ni}$: C, 58.67; H, 3.69; N, 4.28. Found: C, 58.88; H, 3.60; N, 4.26.

Nickel Complex 16b. This complex was synthesized using the procedure described for complex 16a with ligand 10b (108 mg, 0.22 mmol), (DME)NiBr₂ (62 mg, 0.20 mmol), and CH_2Cl_2 (7 mL). Brick

red solid. Yield: 130 mg, 91%. Anal. Calcd for $\text{C}_{36}\text{H}_{32}\text{Br}_2\text{N}_2\text{Ni}$: C, 60.80; H, 4.54; N, 3.94. Found: C, 60.64; H, 4.57; N, 3.99.

ASSOCIATED CONTENT

Supporting Information

The Supporting Information is available free of charge at <https://pubs.acs.org/doi/10.1021/acs.organomet.0c00696>.

NMR spectra of the compounds, supporting figures, characterization of polymers, and X-ray crystallographic data (PDF)

Accession Codes

CCDC 2042450–2042452 contain the supplementary crystallographic data for this paper. These data can be obtained free of charge via www.ccdc.cam.ac.uk/data_request/cif, or by emailing data_request@ccdc.cam.ac.uk, or by contacting The Cambridge Crystallographic Data Centre, 12 Union Road, Cambridge CB2 1EZ, UK; fax: +44 1223 336033.

AUTHOR INFORMATION

Corresponding Authors

Maurice Brookhart – Department of Chemistry, University of Houston, Houston, Texas 77204-5003, United States; Email: mbrookha@central.uh.edu

Olafs Daugulis – Department of Chemistry, University of Houston, Houston, Texas 77204-5003, United States; orcid.org/0000-0003-2642-2992; Email: olafs@uh.edu

Authors

Quan H. Tran – Department of Chemistry, University of Houston, Houston, Texas 77204-5003, United States; orcid.org/0000-0002-7269-3163

Xiqu Wang – Department of Chemistry, University of Houston, Houston, Texas 77204-5003, United States

Complete contact information is available at: <https://pubs.acs.org/10.1021/acs.organomet.0c00696>

Notes

The authors declare no competing financial interest.

ACKNOWLEDGMENTS

This research was supported by the U.S. Department of Energy, Office of Science, Office of Basic Energy Sciences, under Award DE-SC0021403, and by the Welch Foundation (Chair No. E-0044 to O.D. and Grant No. E-1893 to M.B.). The DSC systems used in polymer analysis were funded by the Welch Foundation (Grant No. H-E-0041) through the UH Center of Excellence in Polymer Chemistry.

REFERENCES

- Johnson, L. K.; Killian, C. M.; Brookhart, M. New Pd(II)- and Ni(II)-Based Catalysts for Polymerization of Ethylene and α -Olefins. *J. Am. Chem. Soc.* **1995**, *117*, 6414–6415.
- Johnson, L. K.; Mecking, S.; Brookhart, M. Copolymerization of Ethylene and Propylene with Functionalized Vinyl Monomers by Palladium(II) Catalysts. *J. Am. Chem. Soc.* **1996**, *118*, 267–268.
- Mecking, S.; Johnson, L. K.; Wang, L.; Brookhart, M. Mechanistic Studies on the Palladium-Catalyzed Copolymerization of Ethylene and α -Olefins with Methyl Acrylate. *J. Am. Chem. Soc.* **1998**, *120*, 888–899.
- Ittel, S. D.; Johnson, L. K.; Brookhart, M. Late Metal Catalysts for Ethylene Homo- and Copolymerization. *Chem. Rev.* **2000**, *100*, 1169–1203.

- (5) Rhinehart, J. L.; Mitchell, N. E.; Long, B. K. Enhancing α -Diimine Catalysts for High-Temperature Ethylene Polymerization. *ACS Catal.* **2014**, *4*, 2501–2504.
- (6) Dai, S.; Zhou, S.; Zhang, W.; Chen, C. Systematic Investigations of Ligand Steric Effects on α -Diimine Palladium Catalyzed Olefin Polymerization and Copolymerization. *Macromolecules* **2016**, *49*, 8855–8862.
- (7) Liu, F.-S.; Hu, H.-B.; Xu, Y.; Guo, L.-H.; Zai, S.-B.; Song, K.-M.; Gao, H.-Y.; Zhang, L.; Zhu, F.-M.; Wu, Q. Thermostable α -Diimine Nickel(II) Catalyst for Ethylene Polymerization: Effects of the Substituted Backbone Structure on Catalytic Properties and Branching Structure of Polyethylene. *Macromolecules* **2009**, *42*, 7789–7796.
- (8) Rose, J. M.; Cherian, A. E.; Coates, G. W. Living Polymerization of α -Olefins with an α -Diimine Ni(II) Catalyst: Formation of Well-Defined Ethylene–Propylene Copolymers through Controlled Chain-Walking. *J. Am. Chem. Soc.* **2006**, *128*, 4186–4187.
- (9) Gong, Y.; Li, S.; Gong, Q.; Zhang, S.; Liu, B.; Dai, S. Systematic Investigations of Ligand Steric Effects on α -Diimine Nickel Catalyzed Olefin Polymerization and Copolymerization. *Organometallics* **2019**, *38*, 2919–2926.
- (10) Zhong, L.; Li, G.; Liang, G.; Gao, H.; Wu, Q. Enhancing Thermal Stability and Living Fashion in α -Diimine–Nickel-Catalyzed (Co)polymerization of Ethylene and Polar Monomer by Increasing the Steric Bulk of Ligand Backbone. *Macromolecules* **2017**, *50*, 2675–2682.
- (11) (a) Camacho, D. H.; Salo, E. V.; Ziller, J. W.; Guan, Z. Cyclophane-Based Highly Active Late-Transition-Metal Catalysts for Ethylene Polymerization. *Angew. Chem., Int. Ed.* **2004**, *43*, 1821–1825. (b) Camacho, D. H.; Guan, Z. Living Polymerization of α -Olefins at Elevated Temperatures Catalyzed by a Highly Active and Robust Cyclophane-Based Nickel Catalyst. *Macromolecules* **2005**, *38*, 2544–2546.
- (12) Liu, J.; Chen, D.; Wu, H.; Xiao, Z.; Gao, H.; Zhu, F.; Wu, Q. Polymerization of α -Olefins Using a Camphyl α -Diimine Nickel Catalyst at Elevated Temperature. *Macromolecules* **2014**, *47*, 3325–3331.
- (13) Leung, D. H.; Ziller, J. W.; Guan, Z. Axial Donating Ligands: A New Strategy for Late Transition Metal Olefin Polymerization Catalysis. *J. Am. Chem. Soc.* **2008**, *130*, 7538–7539.
- (14) Meinhard, D.; Wegner, M.; Kipiani, G.; Hearley, A.; Reuter, P.; Fischer, M.; Marti, O.; Rieger, B. New Nickel(II) Diimine Complexes and the Control of Polyethylene Microstructure by Catalyst Design. *J. Am. Chem. Soc.* **2007**, *129*, 9182–9191.
- (15) Zhang, Y.; Wang, C.; Mecking, S.; Jian, Z. Ultrahigh Branching of Main-Chain-Functionalized Polyethylenes by Inverted Insertion Selectivity. *Angew. Chem., Int. Ed.* **2020**, *59*, 14296–14302.
- (16) Rhinehart, J. L.; Brown, L. A.; Long, B. K. A Robust Ni(II) α -Diimine Catalyst for High Temperature Ethylene Polymerization. *J. Am. Chem. Soc.* **2013**, *135*, 16316–16319.
- (17) Zhai, F.; Jordan, R. F. (α -Diimine)nickel Complexes That Contain Menthyl Substituents: Synthesis, Conformational Behavior, and Olefin Polymerization Catalysis. *Organometallics* **2017**, *36*, 2784–2799.
- (18) Chen, Z.; Brookhart, M. Exploring Ethylene/Polar Vinyl Monomer Copolymerizations Using Ni and Pd α -Diimine Catalysts. *Acc. Chem. Res.* **2018**, *51*, 1831–1839.
- (19) Vaccarello, D. N.; O'Connor, K. S.; Iacono, P.; Rose, J. M.; Cherian, A. E.; Coates, G. W. Synthesis of Semicrystalline Polyolefin Materials: Precision Methyl Branching via Stereoretentive Chain Walking. *J. Am. Chem. Soc.* **2018**, *140*, 6208–6211.
- (20) Kanai, Y.; Foro, S.; Plenio, H. Bis(pentiptycenyl)–Diimine–Nickel Complexes for Ethene Polymerization and Copolymerization with Polar Monomers. *Organometallics* **2019**, *38*, 544–551.
- (21) Jia, D.; Zhang, W.; Liu, W.; Wang, L.; Redshaw, C.; Sun, W.-H. Unsymmetrical α -diiminonickel bromide complexes: synthesis, characterization and their catalytic behavior toward ethylene. *Catal. Sci. Technol.* **2013**, *3*, 2737–2745.
- (22) Zhang, D.; Nades, E. T.; Brookhart, M.; Daugulis, O. Synthesis of Highly Branched Polyethylene Using “Sandwich” (8-p-Tolyl naphthyl α -diimine)nickel(II) Catalysts. *Organometallics* **2013**, *32*, 5136–5143.
- (23) Allen, K. E.; Campos, J.; Daugulis, O.; Brookhart, M. Living Polymerization of Ethylene and Copolymerization of Ethylene/Methyl Acrylate Using “Sandwich” Diimine Palladium Catalysts. *ACS Catal.* **2015**, *5*, 456–464.
- (24) Wang, B.; Daugulis, O.; Brookhart, M. Ethylene Polymerization with Ni(II) Diimine Complexes Generated from 8-Halo-1-naphthylamines: The Role of Equilibrating Syn/Anti Diastereomers in Determining Polymer Properties. *Organometallics* **2019**, *38*, 4658–4668.
- (25) Gates, D. P.; Svejda, S. A.; Oñate, E.; Killian, C. M.; Johnson, L. K.; White, P. S.; Brookhart, M. Synthesis of Branched Polyethylene Using (α -Diimine)nickel(II) Catalysts: Influence of Temperature, Ethylene Pressure, and Ligand Structure on Polymer Properties. *Macromolecules* **2000**, *33*, 2320–2334.
- (26) Kocen, A. L.; Brookhart, M.; Daugulis, O. A highly active Ni(II)-triadamantylphosphine catalyst for ultrahigh-molecular-weight polyethylene synthesis. *Nat. Commun.* **2019**, *10*, 438.
- (27) Liang, T.; Goudari, S. B.; Chen, C. A simple and versatile nickel platform for the generation of branched high molecular weight polyolefins. *Nat. Commun.* **2020**, *11*, 372.
- (28) Xia, J.; Zhang, Y.; Kou, S.; Jian, Z. A concerted double-layer steric strategy enables an ultra-highly active nickel catalyst to access ultrahigh molecular weight polyethylenes. *J. Catal.* **2020**, *390*, 30–36.
- (29) Rosa, V.; Avilés, T.; Aullon, G.; Covelo, B.; Lodeiro, C. A New Bis(1-naphthylimino)acenaphthene Compound and Its Pd(II) and Zn(II) Complexes: Synthesis, Characterization, Solid-State Structures and Density Functional Theory Studies on the syn and anti Isomers. *Inorg. Chem.* **2008**, *47*, 7734–7744.
- (30) Svejda, S. A.; Johnson, L. K.; Brookhart, M. Low-temperature spectroscopic observation of chain growth and migratory insertion barriers in (α -diimine)Ni(II) olefin polymerization catalysts. *J. Am. Chem. Soc.* **1999**, *121*, 10634–10635.
- (31) Leatherman, M. D.; Svejda, S. A.; Johnson, L. K.; Brookhart, M. Mechanistic studies of nickel(II) alkyl agostic cations and alkyl ethylene complexes: Investigations of chain propagation and isomerization in (α -diimine)Ni(II)-catalyzed ethylene polymerization. *J. Am. Chem. Soc.* **2003**, *125*, 3068–3081.
- (32) Tempel, D. J.; Johnson, L. K.; Huff, R. L.; White, P. S.; Brookhart, M. Mechanistic studies of Pd(II)- α -diimine-catalyzed olefin polymerizations. *J. Am. Chem. Soc.* **2000**, *122*, 6686–6700.
- (33) Shultz, L. H.; Tempel, D. J.; Brookhart, M. Palladium(II) β agostic alkyl cations and alkyl ethylene complexes: Investigation of polymer chain isomerization mechanisms. *J. Am. Chem. Soc.* **2001**, *123*, 11539–11555.
- (34) Zou, H.; Hu, S.; Huang, H.; Zhu, F.; Wu, Q. Synthesis of bimodal molecular weight distribution polyethylene with α -diimine nickel(II) complexes containing unsym-substituted aryl groups in the presence of methylaluminoxane. *Eur. Polym. J.* **2007**, *43*, 3882–3891.
- (35) Sui, X.; Hong, C.; Pang, W.; Chen, C. Unsymmetrical α -diimine palladium catalysts and their properties in olefin (co)-polymerization. *Mater. Chem. Front.* **2017**, *1*, 967–972.
- (36) Pirkle, W. H.; Selness, S. R. Chiral Recognition Studies: Intra- and Intermolecular 1H{1H}-Nuclear Overhauser Effects as Effective Tools in the Study of Bimolecular Complexes. *J. Org. Chem.* **1995**, *60*, 3252–3256.
- (37) Harada, N.; Saito, A.; Koumura, N.; Uda, H.; de Lange, B.; Jager, W. F.; Wynberg, H.; Feringa, B. L. Chemistry of Unique Chiral Olefins. 1. Synthesis, Enantioresolution, Circular Dichroism, and Theoretical Determination of the Absolute Stereochemistry of trans- and cis-1,1',2,2',3,3',4,4'-Octahydro-4,4'-biphenanthrylidenes. *J. Am. Chem. Soc.* **1997**, *119*, 7241–7248.
- (38) Premasagar, V.; Palaniswamy, V. A.; Eisenbraun, E. J. Methanesulfonic acid catalyzed cyclization of 3-arylpropanoic and 4-arylbutanoic acids to 1-indanones and 1-tetralones. *J. Org. Chem.* **1981**, *46*, 2974–2976.

(39) Hong, W. P.; Iosub, A. V.; Stahl, S. S. Pd-Catalyzed Semmler–Wolff Reactions for the Conversion of Substituted Cyclohexenone Oximes to Primary Anilines. *J. Am. Chem. Soc.* **2013**, *135*, 13664–13667.

(40) Beringer, F. M.; Chang, L. L.; Fenster, A. N.; Rossi, R. R. Synthesis of 4-halophenanthrenes and 4,5-phenanthryleneiodonium salts. *Tetrahedron* **1969**, *25*, 4339–4345.

(41) Klimovica, K.; Kirschbaum, K.; Daugulis, O. Synthesis and Properties of “Sandwich” Diimine-Coinage Metal Ethylene Complexes. *Organometallics* **2016**, *35*, 2938–2943.